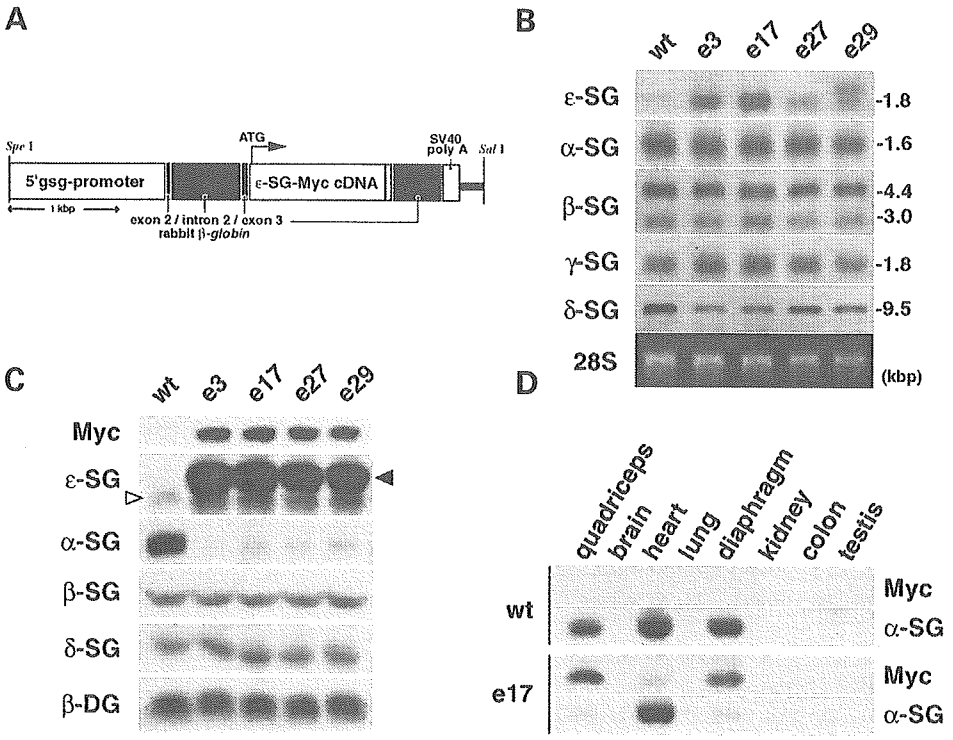

Figure 2. Analyses of SG expression in ε-SG transgenic mice. (**A**) Schematic representation of ε-SG cDNA expression vector. The 1.5 kb mouse *γ-SG* gene promoter and enhancer (5′ gsg-promoter) was connected with rabbit β-*globin* gene fragment (exon 2 intron 2 and exon 3) and SV40 polyadenylation site (26). The c-myc epitope-tagged mouse ε-SG cDNA (ε-SG-Myc cDNA) was inserted into the *Eco*RI site in the β-*globin* exon 3. (**B**) Northern blot analysis of SG expression in skeletal muscle of transgenic mouse lines. Expression of SGs (α-, β-, γ- and δ-SGs) was examined using 2 μg of total RNA prepared from leg muscle of four lines of 5–6-week-old transgenic (e3, e17, e27 and e29) and 5-week-old B6 (wt) mice. The 28S rRNA (28S) is indicated as the internal control. (**C**) Immunoblot analysis of SG expression in the skeletal muscle of transgenic lines. Whole leg muscle lysates of 4–5-week-old transgenic and 5-week-old non-transgenic B6 (wt) mice were subjected to immunoblotting using the 9E10 anti-c-myc monoclonal antibody (Myc) and affinity-purified polyclonal antibodies against ε-SG, α-SG, β-SG and δ-SG. Endogenous ε-SG (open arrowhead) and c-myc-tagged transgene product (solid arrowhead) are distinguished by different molecular sizes on SDS–polyacrylamide electrophoresis. (**D**) Expression of c-myc-tagged ε-SG in transgenic mouse heart. Immunoblots of 8-week-old transgenic (e17) and non-transgenic B6 (wt) mouse tissues were performed with rabbit antibodies against c-myc tag and α-SG.

antibody was used for immunoprecipitation, demonstrating that the ε-SG transgene product was incorporated into the SG subcomplex of the DAP complex at the sarcolemma. Moreover, α-SG was undetectable in this experiment suggesting that the normal adult α-SG complex was replaced by an ε-SG complex composed of ε-, β-, γ- and δ-SGs. No histopathological abnormalities, such as necrosis and regeneration of myocytes, interstitial fibrosis and fatty infiltration, were observed in the muscle of these mice up to 1 year of age. Furthermore, although the *ε-SG* gene is associated with myoclonus–dystonia syndrome (21), there were no abnormal behavior or muscle contractions in mice overexpressing ε-SG.

ε-SG overexpression prevents muscular dystrophy in α-SG-deficient mice

To determine whether increased ε-SG levels could ameliorate the phenotype conferred by α-SG deficiency, the transgenic mouse lines were crossed with α-SG-deficient ($Sgca^{-/-}$) mice, which represents the model for LGMD 2D. Two lines of $Sgca^{-/-}$/tg ($Sgca^{-/-}$/e17 and $Sgca^{-/-}$/e27) were used for most analyses. Immunostaining analysis clearly showed normal expression and localization of β-, γ- and δ-SGs and of sarcospan within the skeletal muscle of the $Sgca^{-/-}$/tg mice (Fig. 4A). Furthermore, immunoprecipitation analysis with anti-c-myc and anti-β-SG antibodies demonstrated normal assembly of the components of the DAP complex in the $Sgca^{-/-}$/e17 muscle (Fig. 4B). These data indicate that ε-SG assembled with β-, γ- and δ-SG in the absence of α-SG and was correctly localized to the sarcolemma.

To determine whether the ε–β–γ–δ complex was functional in muscle, muscle injury was assessed by measuring serum levels of muscle-specific creatine kinase (CK). Ten-week-old $Sgca^{-/-}$ mice had dramatically elevated serum levels of CK, whereas their $Sgca^{-/-}$/tg littermates had CK levels that were similar to those of the wild-type B6 mice (Fig. 5A), indicating a lack of membrane leakage and necrosis in the $Sgca^{-/-}$/tg mice. Muscle membrane integrity was also evaluated by the analysis of serum IgG uptake into muscle fibers (27) (Fig. 5B). Analysis of the tibialis anterior (TA) and rectus femoris muscles of $Sgca^{-/-}$ showed 6.2 ± 0.3% and 7.6 ± 0.8% IgG-positive fibers, respectively, whereas IgG-positive fibers were not observed in the muscles of $Sgca^{-/-}$/tg littermates or of B6 mice. Histopathological examination of the TA, rectus femoris and diaphragm of 10-week-old $Sgca^{-/-}$ mice revealed α-SG deficiency and evidence of muscular dystrophy including degeneration, regeneration, central nucleation and variable sizes of muscle fibers

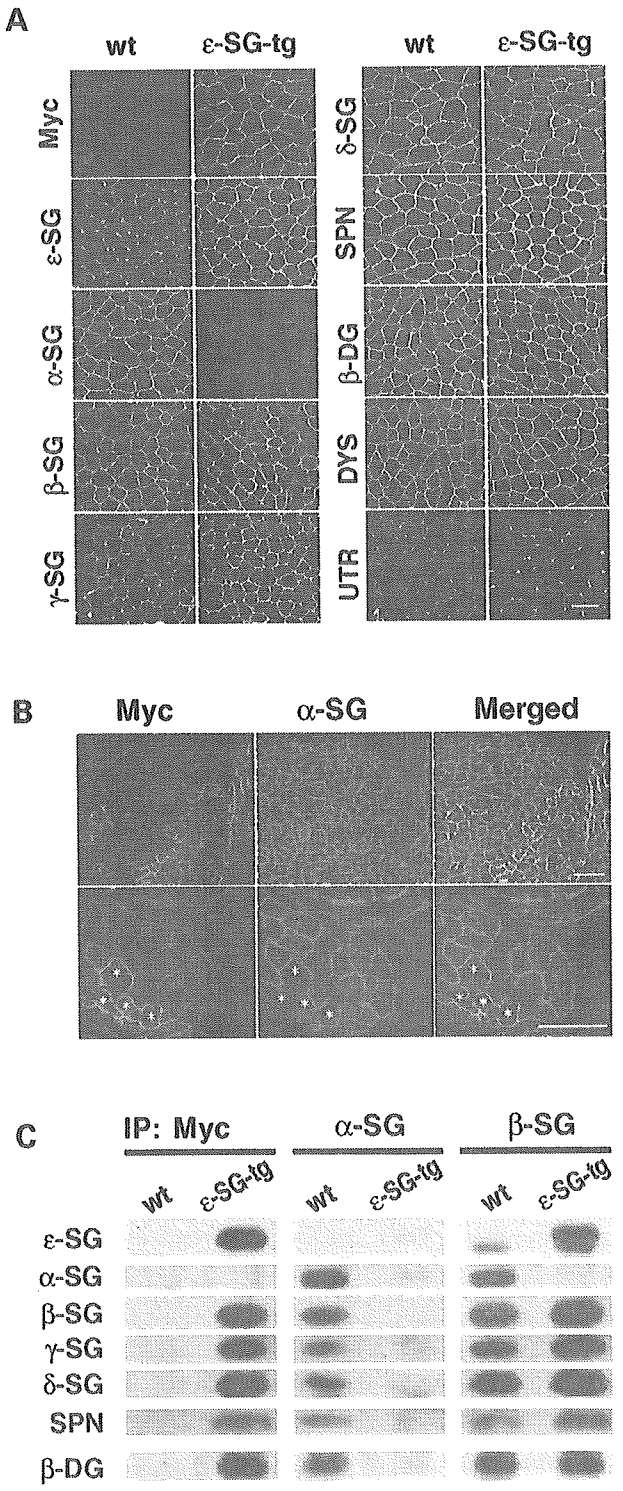

Figure 3. Replacement of α-SG by ε-SG within the SG complex of skeletal muscle in the transgenic mouse. (**A**) Immunohistochemical analysis of dystrophin-associated glycoproteins in the skeletal muscle (quadriceps) expressing ε-SG transgene. Cryosections of a 4-week-old transgenic mouse line, e17, (ε-SG-tg) and non-transgenic B6 (wt) mice were labeled with indirect immunofluorescence using polyclonal antibodies against c-myc (Myc), ε-SG, α-SG, β-SG, γ-SG, δ-SG, sarcospan (SPN), β-dystroglycan (β-DG), dystrophin (DYS) and utrophin (UTR). Bars: 50 μm. (**B**) Expression and localization of transgene product in the transgenic mouse heart. Cryosections of 4-week-old e17 transgenic mouse heart were double stained with anti-c-myc tag (Myc) and anti-α-SG (α-SG) antibodies. Cardiomyocytes with high expression of c-myc-tagged ε-SG (asterisks) show reduced expression levels of α-SG. Bars: 50 μm. (**C**) Molecular composition of SG complex in transgenic mouse muscle. Wheat germ agglutinin (WGA)-bound fraction was prepared from skeletal muscle of 5–6-week-old e17 transgenic (ε-SG-tg) and non-transgenic B6 (wt) mice and used for immunoprecipitation (IP) with Affigel (BioRad)-conjugated polyclonal antibodies against α-SG and β-SG and agarose-conjugated 9E10 anti-c-myc antibody (Santa Cruz). The protein composition of each precipitate was identified by immunoblotting with monoclonal antibodies against α-SG, β-SG, γ-SG, δ-SG and β-DG, rat antibodies against ε-SG and sarcospan (SPN).

(Fig. 5C and D). In contrast, no such signs were detected in *Sgca*$^{-/-}$/e17 mice up to 1 year of age.

Contractile force generation of TA muscles from *Sgca*$^{-/-}$, *Sgca*$^{-/-}$/e17, e17 transgenic and normal B6 mice (Fig. 5E) was measured to evaluate functional recovery. Specific forces in *Sgca*$^{-/-}$/e17 TA muscles were similar to those of B6 and e17 mice and were significantly stronger than those of *Sgca*$^{-/-}$ mice, suggesting that ε–β–γ–δ complexes are physiologically functional. Furthermore, these data suggest that ε-SG acts as a functional homolog of α-SG in muscle and that ε-SG can act as a structural and functional replacement for α-SG in the context of α-SG deficiency.

DISCUSSION

The present study demonstrated that ε-SG can compensate for α-SG deficiency and contribute to the formation of a stable dystrophin–DAP complex in skeletal muscle with amelioration of the dystrophic phenotype. Previous biochemical studies reported that the SG complex reinforces the dystrophin–dystroglycan molecular linkage between the extracellular matrix and cytoskeletal actin (14–16). Observations from the present study are consistent with this report and demonstrate that the ε-SG-containing SG complex (ε–β–γ–δ) has the same ability to stabilize the molecular linkage in skeletal muscle as the normal major SG complex (α–β–γ–δ) in skeletal muscle.

In addition to a structural role, the SG complex may function as a scaffold and as an enzyme in various signal-transduction pathways (7,28,29). Indeed, α-SG possesses a consensus sequence for nucleotide binding in its extracellular domain and was reported to act as an ecto-ATPase, suggesting that the loss of α-SG in sarcoglycanopathies (LGMD 2C–2F) may elevate the extracellular ATP concentration around muscle fibers and result in prolonged stimulation of P2X receptors, calcium overload and muscle cell death (28). However, ε-SG does not possess this conserved sequence for nucleotide binding but can still compensate for α-SG deficiency, suggesting that the loss of the α-SG ecto-ATPase activity is not a major factor in the development of muscular dystrophy in sarcoglycanopathies.

We demonstrated that increased ε-SG expression in skeletal muscle of transgenic mice induces down-regulation of the α-SG protein without changing the mRNA level. Analysis of cardiomyocytes showed that the amount of α-SG protein in the cell membrane was indirectly correlated with that of ε-SG protein. These findings suggest that the amount of

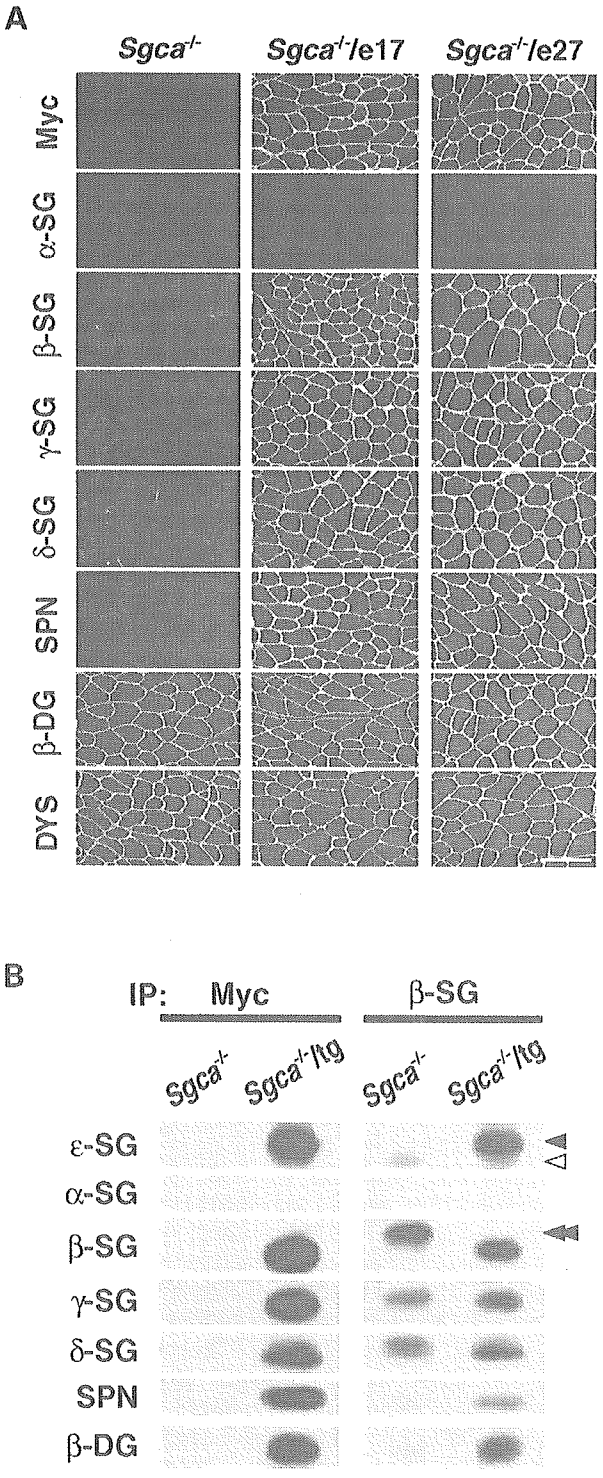

Figure 4. Restoration of SGs and sarcospan at the sarcolemma by ε-SG transgene expression in α-SG-deficient mice. (**A**) Expression and localization of components of SG complex in skeletal muscle of *Sgca*$^{-/-}$/tg were examined by immunohistochemistry. Cryosections of skeletal muscle (quadriceps) of 4-week-old α-SG-deficient (*Sgca*$^{-/-}$) and two lines of *Sgca*$^{-/-}$/tg (*Sgca*$^{-/-}$/e17 and *Sgca*$^{-/-}$/e27) mice underwent indirect immunofluorescent labeling with rabbit antibodies against c-myc (Myc), SGs (ε-, α-, β-, γ- and δ-SGs), sarcospan (SPN), β-dystroglycan (β-DG) and dystrophin (DYS). Bars: 50 μm. Note that *Sgca*$^{-/-}$ mice show marked dystrophic changes in skeletal muscle tissue at around 10 weeks of age (25) but 4-week-old *Sgca*$^{-/-}$ mice do not yet show such changes. (**B**) Reconstruction of the SG complex in skeletal muscle of α-SG-deficient mice by ε-SG transgene expression. WGA-bound fraction of skeletal muscle was prepared from 4-week-old *Sgca*$^{-/-}$ and *Sgca*$^{-/-}$/e17 mice and used for immunoprecipitation (IP) as described in Figure 3. Solid and open arrowheads indicate the bands representing ε-SG transgene product and endogenous ε-SG, respectively. Note that β-SG isolated from *Sgca*$^{-/-}$ skeletal muscle shows higher molecular size (double arrowhead) in comparison with that from *Sgca*$^{-/-}$/tg mice.

α-SG in striated muscle is regulated by post-translational mechanisms. α- and ε-SG proteins may compete in the process of SG complex formation in endoplasmic reticulum (30). Interestingly, a similar reciprocity between ε-SG and α-SG protein expression is found during skeletal muscle development in wild-type mice (31). ε-SG protein is predominant at an early developmental stage, i.e. in myoblasts or myotubes in the formation of axial muscle, and declines after the increase in α-SG protein. However, in the adult, the ε-SG protein is kept at low levels, even when α-SG is completely absent from muscle cells (22,25), suggesting that the amount of ε-SG during skeletal muscle development is regulated at the transcriptional level as is the case of α-SG expression (32).

In the present study, ε-SG levels in normal skeletal muscle tissue were approximately one-tenth those of α-SG. Since ε-SG is highly expressed in vascular smooth muscle, endothelial cells and peripheral nerves, the amount of ε-SG-containing SG complex in skeletal muscle cells would be considerably less than 10%. It is not known whether this minor SG complex has a distinct function in normal skeletal muscle and to what degree it contributes to stabilization of the cell membrane. Loss-of-function mutations of the *ε-SG* gene cause myoclonus–dystonia syndrome but do not result in any obvious abnormalities in skeletal muscle and heart tissues (21). Therefore, the ε-SG-containing SG complex does not appear to be critical for the development and maintenance of the normal striated muscle cell. However, the presence of the minor ε-SG complex may reduce the severity of the phenotype associated with α-SG deficiency.

Previous studies of experimental SG-deficiencies using viral vectors showed that increasing the levels of α-SG, but not the levels of β-, γ- or δ-SG, resulted in cytotoxity in skeletal muscle cells (33–35), possibly secondary to perturbations in SG complex assembly (33). In the present study, several transgenic mouse lines displayed equal levels of ε-SG immunoreactivity, despite the differing levels of ε-SG mRNA. Moreover, the transgene expression did not influence the immunoreactivity levels of other endogenous SGs (β-, γ- and δ-SGs). This suggests that increased synthesis of ε-SG has no adverse effects on SG complex formation and that excess ε-SG may be degraded intracellularly without causing muscle pathology. This situation is similar to the lack of adverse effects observed when utrophin is overexpressed in normal or dystrophin-deficient muscle (36).

In conclusion, these findings show that ε-SG is an excellent replacement for α-SG in mice and suggest that ε-SG expression may be a therapeutic target for the treatment of LGMD 2D in humans. Because ε-SG is encoded in a gene that is maternally imprinted (37,38), reactivation

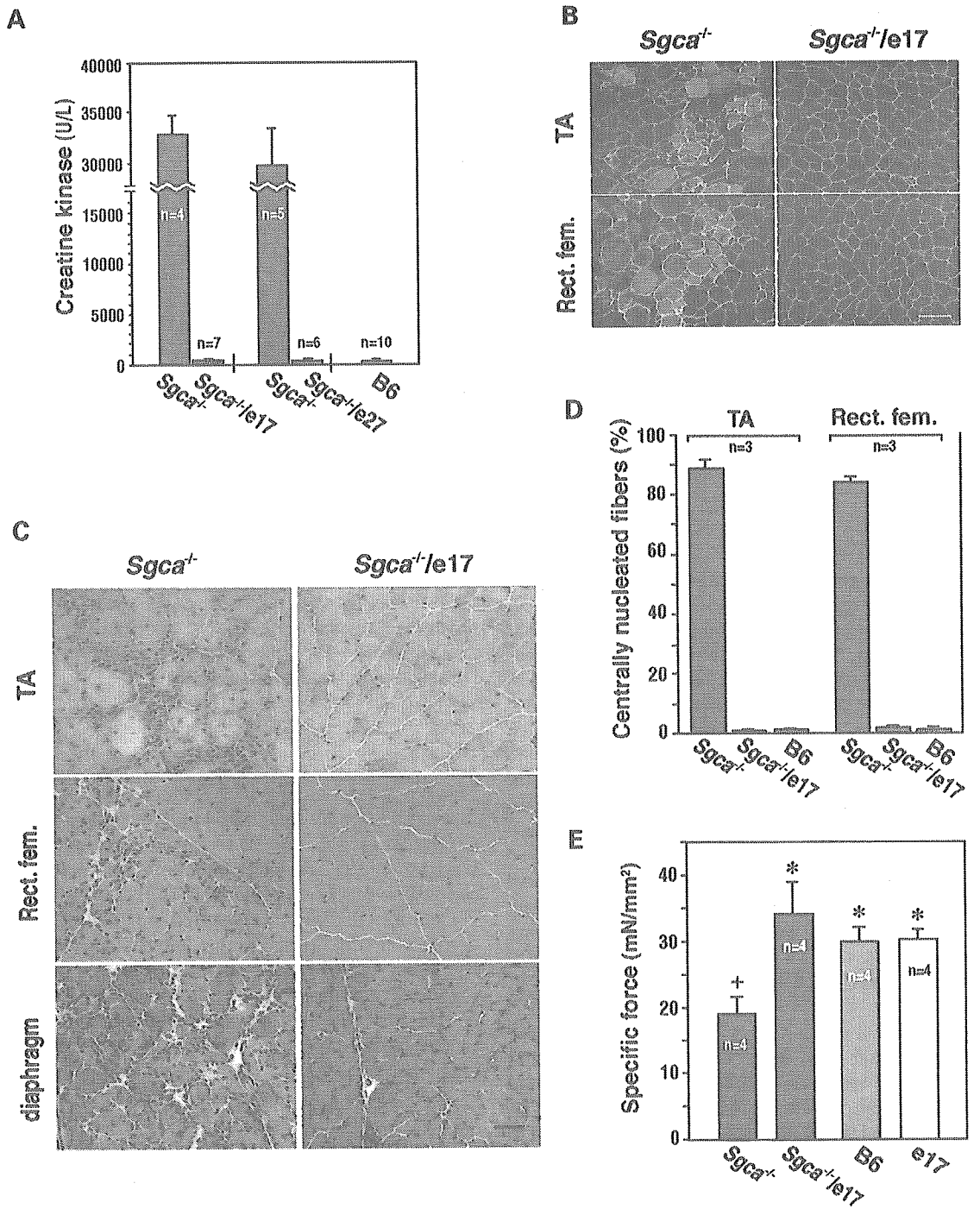

Figure 5. The effect of ε-SG transgene on degeneration of muscle fibers in α-SG deficiency. (**A**) Serum creatine kinase (CK) levels of *Sgca*$^{-/-}$, *Sgca*$^{-/-}$/tg and B6 normal mice at 10 weeks of age. The CK values of *Sgca*$^{-/-}$/tg (*Sgca*$^{-/-}$/e17 and *Sgca*$^{-/-}$/e27) and their littermates (*Sgca*$^{-/-}$) are indicated as adjacent bars. The values of *Sgca*$^{-/-}$/e17 and *Sgca*$^{-/-}$/e27 are statistically significant compared with those of their *Sgca*$^{-/-}$ littermates but not when compared with B6 mice. (**B**) IgG-labeling assay of *Sgca*$^{-/-}$/tg skeletal muscles. Cryosections of tibialis anterior (TA) and rectus femoris muscles were prepared from 10-week-old *Sgca*$^{-/-}$ and *Sgca*$^{-/-}$/e17 mice and were double-stained with the rat monoclonal antibody against laminin-α2 chain (FITC, green) and Cy3-conjugated goat antibody against mouse IgG (red). (**C**) Histological analysis of TA, rectus femoris and diaphragm muscles of 10-week-old *Sgca*$^{-/-}$ and *Sgca*$^{-/-}$/e17 mice by hematoxylin and eosin (H&E) staining. Necrotic fibers, centrally nucleated fibers, cellular infiltrations and fiber size variations are seen in *Sgca*$^{-/-}$ mouse but not in *Sgca*$^{-/-}$/e17 littermate. Bars: 50 μm. (**D**) A marked reduction in number of centrally nucleated muscle fibers in *Sgca*$^{-/-}$/e17 mice. Centrally nucleated fibers were counted in H&E-stained transverse cryosections from 10-week-old *Sgca*$^{-/-}$/e17 mice and their *Sgca*$^{-/-}$ littermates. Age-matched B6 was examined as reference for normal mice. Percentages of the fiber in *Sgca*$^{-/-}$/e17 hind limb muscles are significantly different when compared with those of *Sgca*$^{-/-}$ littermates but not when compared with those of B6 mice. (**E**) Comparison of specific force generation of TA muscles from *Sgca*$^{-/-}$ and *Sgca*$^{-/-}$/tg mice. Differences in specific force generation among 9-week-old *Sgca*$^{-/-}$ and *Sgca*$^{-/-}$/e17 littermates, and age-matched B6 and e17 transgenic mice are determined by Fisher's PLSD. $^{*}P < 0.05$ compared with *Sgca*$^{-/-}$ mice; $+P < 0.05$ compared with *Sgca*$^{-/-}$/e17 mice.

of the silenced maternal allele could potentially be achieved pharmacologically (39,40). It will be interesting to try to find and develop strategies for up-regulation of the endogenous ε-SG in striated muscle in the future.

MATERIALS AND METHODS

ε-SG cDNA.

Full-length mouse ε-SG (nucleotides 10–1404 of GenBank accession no. AF031919) was cloned from a mouse skeletal muscle cDNA library (Clontech, Palo Alto, CA, USA) by polymerase chain reaction (PCR), as described previously (32). In order to add the c-myc-epitope sequence at the C-terminal of ε-SG, the cloned cDNA was subjected to repetitive PCR with reverse primers tagged with the c-myc-epitope sequence. The final cDNA product (1.3 kb) was cloned into pCR2.1 (Invitrogen Life Technologies, Carlsbad, CA, USA) and sequenced, as described previously (19).

Transgenic mice

A transgene vector was generated by replacement of the EGFP cDNA with the c-myc-tagged mouse ε-SG cDNA in the 5′-gsg (mouse γ-*SG* promoter/enhancer)-containing expression construct (26). The linear transgene construct (4.4 kb) was excised by digestion with *Spe*I and *Sal*I prior to microinjection into pronuclei of fertilized eggs of C57BL/6 (B6) mice. Genomic DNA was extracted from tails and screened by PCR for integration of the transgene. The ε-SG transgenic (heterozygous) male mice were bred to α-SG-deficient ($Sgca^{-/-}$) female mice (22) supplied from the Burnham Institute (La Jolla, CA, USA). The resulting male mice (transgenic-$Sgca^{+/-}$) were bred with $Sgca^{-/-}$ female mice and their offspring, transgenic-$Sgca^{-/-}$ and $Sgca^{-/-}$ mice, were used for analysis. The transgenic-$Sgca^{-/-}$ male mice were further bred with $Sgca^{-/-}$ female mice, and their offspring were used for analysis with an IgG-staining assay, quantification of centrally nucleated fibers and measurement of muscle contraction.

Tetanic force of TA muscles from 9-week-old $Sgca^{-/-}$ and $Sgca^{-/-}$/e17 littermates and age-matched e17 transgenic and B6 normal mice was measured at a stimulus frequency of 126 Hz, as described previously (41). Serum CK levels of the mice were measured by the SRL Laboratory (Tokyo, Japan). All animal handling procedures were performed in accordance with a protocol approved by the National Institute of Neuroscience, NCNP, Japan.

Northern blot analysis

Two micrograms of total RNA were prepared from leg muscle of 5-week-old transgenic mice and wild-type (B6) mice and were separated by formaldehyde/agarose gel electrophoresis before transferring onto Nylon Membranes (Roche Diagnostics, Mannheim, Germany). Digoxigenin (DIG)-labeled SG RNA probes were generated by *in vitro* transcription using T7 RNA polymerase and were used for the detection of SG mRNAs according to the manufacturer's protocol.

Antibodies

Mouse monoclonal antibodies against α-SG (NCL-a-SARC), β-SG (NCL-b-SARC), γ-SG (NCL-g-SARC) and β-dystroglycan (NCL-b-DG) were purchased from Novo Castra Laboratories (Newcastle-upon-Tyne, UK). A mouse monoclonal antibody against c-myc (9E10) and a 9E10-agarose-coupled antibody were purchased from Santa Cruz Biotechnology (Santa Cruz, CA, USA). A rat monoclonal antibody against the laminin-α2 chain (4H8-2) was purchased from Alexis (Läufelfingen, Switzerland). Anti-c-myc rabbit antibodies were purchased from Upstate Biotechnology (Lake Placid, NY, USA) and MBL (Nagoya, Japan). A mouse monoclonal antibody against δ-SG (DSG-1) and affinity-purified rabbit antibodies against α-SG, β-SG, mouse sarcospan, β-dystroglycan and utrophin (UT-2) were generated (16,19), and immunoprecipitation and immunoblotting were performed with these antibodies as previously described (19).

An anti-SG rabbit antibody, which recognizes homologous regions of α- and ε-SG (α/ε-SG antibody), was prepared by affinity-purification. The anti-ε-SG cytoplasmic region (ε-SGcyt) antiserum was affinity-purified using recombinant glutathione S-transferase (GST) and GST-ε-SGcyt fusion protein (19). This anti-ε-SGcyt antibody was then further purified using a GST-fusion protein with the α-SG cytoplasmic region (16). Quantification of α/ε-SG immunoreactivity in immunoblot analysis (Fig. 1) was performed using an image analyzer (Lumi-Imager; Roche Diagnostics).

Histology

Muscles were immersed in Tragacanth Gum (Wako, Tokyo, Japan) and rapidly frozen in liquid nitrogen-cooled isopentane. Cryosections were subjected to hematoxylin and eosin (H&E) staining or to indirect immunofluorescent staining under conditions described previously (42).

Centrally nucleated fibers were counted in transverse H&E cryosections of TA and rectus femoris muscles from $Sgca^{-/-}$ and $Sgca^{-/-}$/e17 littermates and from B6 normal mice.

Serum protein IgG that infiltrated into dystrophic muscle fibers was detected by immunofluorescent labeling (27). Labeling was performed on 3.5% formaldehyde-fixed 8 μm transverse cryosections using a Cy3-conjugated goat antibody against mouse IgG (Jackson ImmunoResearch, West Grove, PA, USA). To identify muscle fibers, these sections were double-stained with a rat monoclonal antibody against laminin-α2 chain (4H8-2), as described previously (42). Fluorescent signal on the cryosections was observed under a confocal laser scanning microscope (Leica TCS SP; Leica, Heidelberg, Germany). IgG-positive and -negative fibers on the micrographs of the stained muscle sections were counted.

Double-staining of heart cryosections from e17 transgenic mice were performed using rabbit antibodies against the c-myc epitope tag and α-SG. The heart cryosections were subsequently reacted with an anti-c-myc rabbit antibody (MBL) and a FITC-conjugated goat Fab (monovalent) antibody fragment against rabbit IgG. After washing with phosphate-buffered saline, these sections were reacted with Alexa568-conjugated affinity purified rabbit antibody against α-SG.

Statistical analysis

The data shown in Fig. 5A, D and E and IgG-staining of muscle fibers are expressed as mean ± SEM. If a significant F ratio was detected after analysis of variance, comparisons among each group were performed using Fisher's PLSD. A P-value of <0.05 was considered to be statistically significant.

ACKNOWLEDGEMENTS

We thank N. Noguchi for providing the 5′-gsg-promoter/enhancer cDNA and T. Sasaoka for advice on maintenance and care of mice. This study was supported by Grants-in-Aid for Center of Excellence (COE), Research on Nervous and Mental Disorders (13B-1), and Health Sciences Research Grants for Research on Psychiatric and Neurological Diseases and Mental Health (H12-kokoro-025), the Human Genome and Gene Therapy (H13-genome-001) from the Ministry of Health, Labor and Welfare of Japan, and a Grant-in-Aid for Scientific Research (B) from the Ministry of Education, Science, Sports and Culture of Japan (to M.I., Y.M. and S.T.) and from the National Institutes of Health and the Muscular Dystrophy Association, USA (to E.E.).

REFERENCES

1. Ervasti, J.M., Ohlendieck, K., Kahl, S.D., Gaver, M.G. and Campbell, K.P. (1990) Deficiency of a glycoprotein component of the dystrophin complex in dystrophic muscle. *Nature*, **345**, 315–319.
2. Yoshida, M. and Ozawa, E. (1990) Glycoprotein complex anchoring dystrophin to sarcolemma. *J. Biochem.(Tokyo)*, **108**, 748–752.
3. Ozawa, E., Noguchi, S., Mizuno, Y., Hagiwara, Y. and Yoshida, M. (1998) From dystrophinopathy to sarcoglycanopathy: evolution of a concept of muscular dystrophy. *Muscle Nerve*, **21**, 421–438.
4. Suzuki, A., Yoshida, M., Hayashi, K., Mizuno, Y., Hagiwara, Y. and Ozawa, E. (1994) Molecular organization at the glycoprotein-complex-binding site of dystrophin. Three dystrophin-associated proteins bind directly to the carboxy-terminal portion of dystrophin. *Eur. J. Biochem.*, **220**, 283–292.
5. Ozawa, E., Imamura, M., Noguchi, S. and Yoshida, M. (2000) Dystrophinopathy and sarcoglycanopathy, *Neurosci. News*, **3**, 13–19.
6. Yoshida, M., Suzuki, A., Yamamoto, H., Noguchi, S., Mizuno, Y. and Ozawa, E. (1994) Dissociation of the complex of dystrophin and its associated proteins into several unique groups by *n*-octyl β-D-glucoside, *Eur. J. Biochem.*, **222**, 1055–1061.
7. Yoshida, M., Hama, H., Ishikawa-Sakurai, M., Imamura, M., Mizuno, Y., Araishi, K., Wakabayashi-Takai, E., Noguchi, S., Sasaoka, T. and Ozawa, E. (2000) Biochemical evidence for association of dystrobrevin with the sarcoglycan–sarcospan complex as a basis for understanding sarcoglycanopathy. *Hum. Mol. Genet.*, **9**, 1033–1040.
8. Mizuno, Y., Noguchi, S., Yamamoto, H., Yoshida, M., Suzuki, A., Hagiwara, Y., Hayashi, Y.K., Arahata, K., Nonaka, I., Hirai, S. *et al.* (1994) Selective defect of sarcoglycan complex in severe childhood autosomal recessive muscular dystrophy muscle. *Biochem. Biophys. Res. Commun.*, **203**, 979–983.
9. Roberds, S.L., Leturcq, F., Allamand, V., Piccolo, F., Jeanpierre, M., Anderson, R.D., Lim, L.E., Lee, J.C., Tomé, F.M., Romero, N.B. *et al.* (1994) Missense mutations in the *adhalin* gene linked to autosomal recessive muscular dystrophy, *Cell*, **78**, 625–633.
10. Lim, L.E., Duclos, F., Broux, O., Bourg, N., Sunada, Y., Allamand, V., Meyer, J., Richard, I., Moomaw, C., Slaughter, C. *et al.* (1995) β-Sarcoglycan: characterization and role in limb-girdle muscular dystrophy linked to 4q12. *Nat. Genet.*, **11**, 257–265.
11. Bönnemann, C.G., Modi, R., Noguchi, S., Mizuno, Y., Yoshida, M., Gussoni, E., McNally, E.M., Duggan, D.J., Angelini, C., Hoffman, E.P. *et al.* (1995) β-Sarcoglycan (A3b) mutations cause autosomal recessive muscular dystrophy with loss of the sarcoglycan complex. *Nat. Genet.*, **11**, 266–273.
12. Noguchi, S., McNally, E.M., Ben Othmane, K., Hagiwara, Y., Mizuno, Y., Yoshida, M., Yamamoto, H., Bönnemann, C.G., Gussoni, E., Denton, P.H. *et al.* (1995) Mutations in the dystrophin-associated protein γ-sarcoglycan in chromosome 13 muscular dystrophy, *Science*, **270**, 819–822.
13. Nigro, V., Moreira, E.S., Piluso, G., Vainzof, M., Belsito, A., Politano, L., Puca, A.A., Passos-Bueno, M.R. and Zatz, M. (1996) Autosomal recessive limb-girdle muscular dystrophy, LGMD2F, is caused by a mutation in the δ-*sarcoglycan* gene. *Nat. Genet.*, **14**, 195–198.
14. Iwata, Y., Nakamura, H., Mizuno, Y., Yoshida, M., Ozawa, E. and Shigekawa, M. (1993) Defective association of dystrophin with sarcolemmal glycoproteins in the cardiomyopathic hamster heart. *FEBS Lett.*, **329**, 227–231.
15. Holt, K.H., Lim, L.E., Straub, V., Venzke, D.P., Duclos, F., Anderson, R.D., Davidson, B.L. and Campbell K.P. (1998) Functional rescue of the sarcoglycan complex in the BIO 14.6 hamster using δ-*sarcoglycan* gene transfer. *Mol. Cell*, **1**, 841–848.
16. Araishi, K., Sasaoka, T., Imamura, M., Noguchi, S., Hama, H., Wakabayashi, E., Yoshida, M., Hori, T. and Ozawa, E. (1999) Loss of the sarcoglycan complex and sarcospan leads to muscular dystrophy in β-sarcoglycan-deficient mice, *Hum. Mol. Genet.*, **8**, 1589–1598.
17. Ettinger, A.J., Feng, G. and Sanes, J.R. (1997) ε-Sarcoglycan, a broadly expressed homologue of the gene mutated in limb-girdle muscular dystrophy 2D. *J. Biol. Chem.*, **272**, 32534–32538.
18. McNally, E.M., Ly, C.T. and Kunkel, L.M. (1998) Human ε-sarcoglycan is highly related to α-sarcoglycan (adhalin), the limb girdle muscular dystrophy 2D gene. *FEBS Lett.*, **422**, 27–32.
19. Imamura, M., Araishi, K., Noguchi, S. and Ozawa, E. (2000) A sarcoglycan–dystroglycan complex anchors Dp116 and utrophin in the peripheral nervous system. *Hum. Mol. Genet.*, **9**, 3091–3100.
20. Nishiyama, A., Endo, T., Takeda, S. and Imamura, M. (2004) Identification and characterization of ε-sarcoglycans in the central nervous system. *Brain Res. Mol. Brain Res.*, **125**, 1–12.
21. Zimprich, A., Grabowski, M., Asmus, F., Naumann, M., Berg, D., Bertram, M., Scheidtmann, K., Kern, P., Winkelmann, J., Muller-Myhsok, B. *et al.* (2001) Mutations in the gene encoding ε-sarcoglycan cause myoclonus–dystonia syndrome. *Nat. Genet.*, **29**, 66–69.
22. Liu, L.A. and Engvall, E. (1999) Sarcoglycan isoform in skeletal muscle. *J. Biol. Chem.*, **274**, 38171–38176.
23. Durbeej, M. and Campbell, K.P. (1999) Biochemical characterization of the epithelial dystroglycan complex. *J. Biol. Chem.*, **274**, 26609–26616.
24. Durbeej, M., Cohn, R.D., Hrstka, R.F., Moore, S.A., Allamand, V., Davidson, B.L., Williamson, R.A. and Campbell, K.P. (2000) Disruption of the β-*sarcoglycan* gene reveals pathogenetic complexity of limb-girdle muscular dystrophy type 2E. *Mol. Cell*, **5**, 141–151.
25. Duclos, F., Straub, V., Moore, S.A., Venzke, D.P., Hrstka, R.F., Crosbie, R.H., Durbeej, M., Lebakken, C.S., Ettinger, A.J., van der Meulen, J. *et al.* (1998) Progressive muscular dystrophy in α-sarcoglycan-deficient mice. *J. Cell Biol.*, **142**, 1461–1471.
26. Noguchi, S., Wakabayashi-Takai, E., Sasaoka, T. and Ozawa, E. (2001) Analysis of the spatial, temporal and tissue-specific transcription of γ-*sarcoglycan* gene using a transgenic mouse. *FEBS Lett.*, **495**, 77–81.
27. Straub, V., Rafael, J.A., Chamberlain, J.S. and Campbell, K.P. (1997) Animal models for muscular dystrophy show different pattern of sarcolemmal disruption. *J. Cell Biol.*, **139**, 375–385.
28. Betto, R., Senter, L., Ceoldo, S., Tarricone, E., Biral, D. and Salviati, G. (1999) Ecto-ATPase activity of α-sarcoglycan (Adhalin). *J. Biol. Chem.* **274**, 7907–7912.
29. Sandona., D., Gastaldello, S., Martinello, T. and Betto, R. (2004) Characterization of the ATP-hydrolysing activity of α-sarcoglycan. *Biochem. J.* **381**, 105–112.
30. Noguchi, S. Wakabayashi, E., Imamura, M., Yoshida, M. and Ozawa, E. (2000) Formation of sarcoglycan complex with differentiation in cultured myocytes. *Eur. J. Biochem.* **267**, 640–648.
31. Straub, V., Ettinger, J.A., Durbeej, M., Venzke, D.P., Cutshall, S., Sanes, J.R. and Campbell, K.P. (1999) ε-Sarcoglycan replaces α-sarcoglycan in smooth muscle to form a unique dystrophin–glycoprotein complex. *J. Biol. Chem.* **274**, 27989–27996.
32. Noguchi, S. Wakabayashi, E., Imamura, M., Yoshida, M. and Ozawa, E. (1999) Developmental expression of *sarcoglycan* gene products in cultured myocytes. *Biochem. Biophys. Res. Commun.* **262**, 88–93.
33. Dressman, D., Araishi, K., Imamura, M., Sasaoka, T., Liu, L.A., Engvall, E. and Hoffman, E.P. (2002) Delivery of α- and β-sarcoglycan

by recombinant adeno-associated virus: efficient rescue of muscle, but differential toxicity. *Hum. Gene Ther.*, **13**, 1631–1646.
34.. Cordier, L., Hack, A.A., Scott, M.O., Barton-Davis, E.R., Gao, G., Wilson, J.M., McNally, E.M. and Sweeney, H.L. (2000) Rescue of skeletal muscles of γ-sarcoglycan-deficient mice with adeno-associated virus-mediated gene transfer. *Mol. Ther.*, **1**, 119–129.
35. Xiao, X., Li, J., Tsao, Y.P., Dressman, D., Hoffman, E.P. and Watchko, J.F. (2000) Full functional rescue of a complete muscle (TA) in dystrophic hamsters by adeno-associated virus vector-directed gene therapy. *J. Virol.*, **74**, 1436–1442.
36. Tinsley, J., Deconinck, N., Fisher, R., Kahn, D., Phelps, S., Gillis, J.-M. and Davies, K. Expression of full-length utrophin prevent muscular dystroph in mdx mice. (1998) *Nat. Med.*, **4**, 1441–1444.
37. Piras, G., El Kharroubi, A., Kozlov, S., Escalante-Alcalde, D., Hernandez, L., Copeland, N.G., Gilbert, D.J., Jenkins, N.A. and Stewart, C.L. (2000) *Zac1* (*Lot1*), a potential tumor suppressor gene, and the gene for ε-sarcoglycan are maternally imprinted genes: identification by a subtractive screen of novel uniparental fibroblast line. *Mol. Cell. Biol.*, **20**, 3308–3315.
38. Müller, B., Hedrich, K., Kock, N., Dragasevic, N., Svetel, M., Garrels, J., Landt, O., Nitschke, M., Pramstaller, P.P., Reik, W. *et al.* (2002) Evidence that paternal expression of the ε-*sarcoglycan* gene accounts for reduced penetrance in myoclonus–dystonia. *Am. J. Hum. Genet.*, **71**, 1303–1311.
39. Doerksen, T., Benoit, G. and Trasler, J.M. (2000) Deoxyribonucleic acid hypomethylation of male germ cells by mitotic and meiotic exposure to 5-azacytidine I associated with altered testicular histology. *Endocrinology*, **141**, 3235–3244.
40. Kharroubi, E.I., Piras, G. and Stewart, C.L. (2001) DNA demethylation reactivates a subset of imprinted genes in uniparental mouse embryonic fibroblasts. *J. Biol. Chem.*, **276**, 8674–8680.
41. Hosaka, Y., Yokota, T., Miyagoe-Suzuki, Y., Yuasa, K., Imamura, M., Matsuda, R., Ikemoto, T., Kameya, S. and Takeda, S. (2002) α1-Syntrophin-deficient skeletal muscle exhibits hypertrophy and aberrant formation of neuromuscular junctions during regeneration. *J. Cell Biol.*, **158**, 1097–1107.
42. Sasaoka, T., Imamura, M., Araishi, K., Noguchi, S., Mizuno, Y., Tkagoshi, N., Hama, H., Wakabayashi-Takai, E., Yoshimoto-matsuda, Y., Nonaka, I. *et al.* (2003) Pathological analysis of muscle hypertrophy and degeneration in muscular dystrophy in γ-sarcoglycan-deficient mice. *Neuromuscul. Disord.*, **13**, 193–206.

THE JOURNAL OF GENE MEDICINE
J Gene Med 2005; 7: 237–248.
Published online 10 November 2004 in Wiley InterScience (www.interscience.wiley.com). **DOI:** 10.1002/jgm.651

RESEARCH ARTICLE

The utrophin promoter A drives high expression of the transgenic *LacZ* gene in liver, testis, colon, submandibular gland, and small intestine

Joji Takahashi[1,2]
Yuka Itoh[1]
Keita Fujimori[3]
Michihiro Imamura[1]
Yoshihiro Wakayama[2]
Yuko Miyagoe-Suzuki[1]
Shin'ichi Takeda[1]*

[1]*Department of Molecular Therapy, National Institute of Neuroscience, National Center of Neurology and Psychiatry, 4-1-1 Ogawa-higashi, Kodaira, Tokyo 187-8502, Japan*

[2]*Department of Neurology, Showa University Fujigaoka Hospital, 1-30 Fujigaoka, Aoba-ku, Yokohama 227-8501, Japan*

[3]*Department of Ophthalmology, Akita University School of Medicine, 1-1-1 Hondo, Akita 010-8543, Japan*

*Correspondence to:
Shin'ichi Takeda, Department of Molecular Therapy, National Institute of Neuroscience, National Center of Neurology and Psychiatry, 4-1-1 Ogawa-higashi, Kodaira, Tokyo 187-8502, Japan. E-mail: takeda@ncnp.go.jp

Received: 30 March 2004
Revised: 31 May 2004
Accepted: 1 June 2004

Abstract

Background Duchenne muscular dystrophy (DMD) is caused by the absence of the muscle cytoskeletal protein dystrophin. Utrophin is an autosomal homologue of dystrophin, and overexpression of the protein is expected to compensate for the defect of dystrophin. The *utrophin* gene has two promoters, A and B, and promoter A of the *utrophin* gene is a possible target of pharmacological interventions for DMD because A-utrophin is up-regulated in dystrophin-deficient *mdx* skeletal and cardiac muscles. To investigate the utrophin promoter A activity *in vivo*, we generated nuclear localization signal-tagged *LacZ* transgenic mice, where the *LacZ* gene was driven by the 5-kb flanking region of the A-*utrophin* gene.

Methods Four transgenic lines were established by mating four independent founders with C57BL/6J mice. The levels of mRNA for β-galactosidase in several tissues were examined by RT-PCR. Cryosections from several tissues were stained with hematoxylin and eosin (H&E) and with 5-bromo-4-chloro-3-indolyl-β-D-galactopyranoside (X-Gal).

Results The 5-kb upstream region of the A-*utrophin* gene showed high transcriptional activity in liver, testis, colon, submandibular gland, and small intestine, consistent with the endogenous expression of utrophin protein. Surprisingly, the levels of both β-gal protein and mRNA for the transgene in cardiac and skeletal muscles were extremely low, even in nuclei near the neuromuscular junctions. These results indicate that the regulation of the *utrophin* gene in striated muscle is different from that in non-muscle tissues.

Conclusions Our results clearly showed that the utrophin A promoter is not sufficient to drive expression in muscle, but other regulatory elements are required. Copyright © 2004 John Wiley & Sons, Ltd.

Keywords Duchenne muscular dystrophy; dystrophin; utrophin; promoter; β-galactosidase

Introduction

Duchenne muscular dystrophy (DMD) is an X-linked lethal disorder caused by a defect in the *DMD* gene, which encodes a large cytoskeletal protein, dystrophin [1]. Dystrophin is normally expressed on the subsarcolemma and interacts with dystrophin-associated-proteins (DAPs) [2–5]. These proteins link the cytoskeleton of myofibers to the extracellular matrix and maintain the integrity of muscle fibers. The

lack of dystrophin in DMD prevents the assembly of DAPs on the sarcolemma and leads to massive muscle necrosis, resulting in cardiomyopathy and early death.

Utrophin is a 395-kDa cytoskeletal protein with a high degree of amino acid identity with dystrophin [6,7]. It is ubiquitously expressed in most tissues. In embryonic and neonatal skeletal muscles, it is expressed both synaptically and extra-synaptically. In adult skeletal muscle, it is found only at the postsynaptic membrane of the neuromuscular junction (NMJ) and the myotendinous junction [8,9]. During muscle regeneration, it transiently reappears at the sarcolemma of immature muscle fibers [10].

Previous transgenic experiments showed that overexpression of utrophin at the sarcolemma compensates for the lack of dystrophin function and ameliorates dystrophic phenotypes in dystrophin-deficient *mdx* mice [11–13]. Similarly, it has been shown that adenovirally induced utrophin improves dystrophic changes in *mdx* mice [14]. We previously reported that adenovirally transferred β-galactosidase (β-gal) expression evoked up-regulation of endogenous utrophin, resulting in partial amelioration of dystrophic phenotypes of dystrophin-deficient *mdx* muscle [15]. These findings suggest that up-regulation of endogenous utrophin is an alternative strategy for DMD therapy.

Transcriptional regulation of the *utrophin* gene is more complicated than previously pictured. There are two full-length utrophin mRNAs, A and B, with different N termini, which are driven by two distinct promoters [16,17]. Further, it has been shown that transcription of A-utrophin is augmented by an intronic enhancer [18]. Both A- and B-utrophin mRNA are expressed in a tissue-specific manner, and an immunohistochemical study showed that A-utrophin is expressed at the NMJ, choroid plexus, pia mater, and renal glomerulus and tubule, and is up-regulated in regenerating muscle and in *mdx* muscle [19,20]. On the other hand, B-utrophin is expressed in vascular endothelial cells [20]. Several short utrophin isoforms have also been reported, as found in dystrophin [21]. Importantly, there is some evidence suggesting that the expression of utrophin is regulated at multiple levels, including transcription, targeting of transcripts and regulation of mRNA stability. In particular, the stability of transcripts is regulated mainly by the interaction of the 3′-untranslated region (3′-UTR) of utrophin mRNA with sequence-specific RNA binding proteins [22,23].

We previously reported that local administration of recombinant interleukin-6 (rIL-6) elevated the level of utrophin at the sarcolemma in dystrophin-deficient *mdx* muscle, although the effects continued for only a short time [24]. To further elucidate the transcriptional regulation of utrophin in skeletal muscle, we generated transgenic mice in which the *LacZ* gene is driven by the 5320-bp 5′-flanking region containing the utrophin A core promoter. Here we show that the 5-kb upstream region of A-utrophin drives strong expression of nuclear localization signal (nls)-tagged β-gal expression in cells adjacent to basal lamina in liver, testis, colon, submandibular gland, and small intestine, but shows extremely low transcriptional activity in skeletal and cardiac muscles.

Materials and methods

Construction of the transgene and generation of transgenic mice

Genomic fragments containing the 5′ end of the mouse A-*utrophin* gene were cloned from a 129Sv mouse genomic library (Stratagene). One clone contained the 5320-bp 5′-flanking region of the A-*utrophin* gene, the complete exon 1A and the first 59 bp of the exon 2 UTR. The genomic fragment was fused in-frame to an nls (from SV40T antigen)-tagged *LacZ* gene [25] (pCMVb, Clontech) followed by a rabbit β-globin poly A signal in Bluescript II (Stratagene) (see also Figures 1A and 1B). The DNA fragment containing the transgene expression cassette was purified from an agarose gel and injected into C57BL/6J fertilized eggs by GenCom (Machida, Tokyo, Japan) (see also Figure 1C). We obtained four transgenic F_0 (utrophin promoter A/nls-LacZ transgenic (Tg)) mice, and four transgenic lines were established by mating founders with C57BL/6J mice (B6). To obtain transgenic *mdx* (Tg/*mdx*) male mice, transgene-positive F_1 males were mated with *mdx* females (also see Figure 1D).

Animals

B6 and *mdx* mice aged 8–10 weeks, Tg mice and their wild-type littermates aged 3–18 weeks, and Tg/*mdx* mice aged 2–4 weeks were used. All animals were housed in a separate room with controlled temperature (20–22 °C) and under an artificial lighting regime (12 h light/12 h dark). Tg mice were 5 weeks old and Tg/*mdx* mice were 2 weeks old when they were anesthetized by inhalation of diethyl ether (Wako Chemicals, Japan), and cardiotoxin or rIL-6 was injected into their tibialis anterior (TA) muscles. Animals were sacrificed by cervical dislocation. All protocols were approved by the Institutional Animal Care and Use Committee of the National Institute of Neuroscience and were performed in compliance with the "Guide for the Care and Use of Animals" of the Division of Laboratory Animal Resources.

Genotyping

Tg mice were screened by Southern blot analysis of genomic DNA from their tails. Genomic DNA was isolated using a lysis buffer (50 mM Tris-HCl, pH 8.0, 0.1 M NaCl, 20 mM EDTA, 1% SDS) with proteinase K (0.15 mg/ml) and pronase E (1 mg/ml) digestion. Genomic DNA (10 μg) was digested by *BamH* I, separated on a 0.8% agarose gel, and transferred onto Hybond-N^+ membranes (Amersham Biosciences, UK). A 3072-bp DNA fragment of the *LacZ* gene was labeled with ^{32}P-dCTP as a Southern

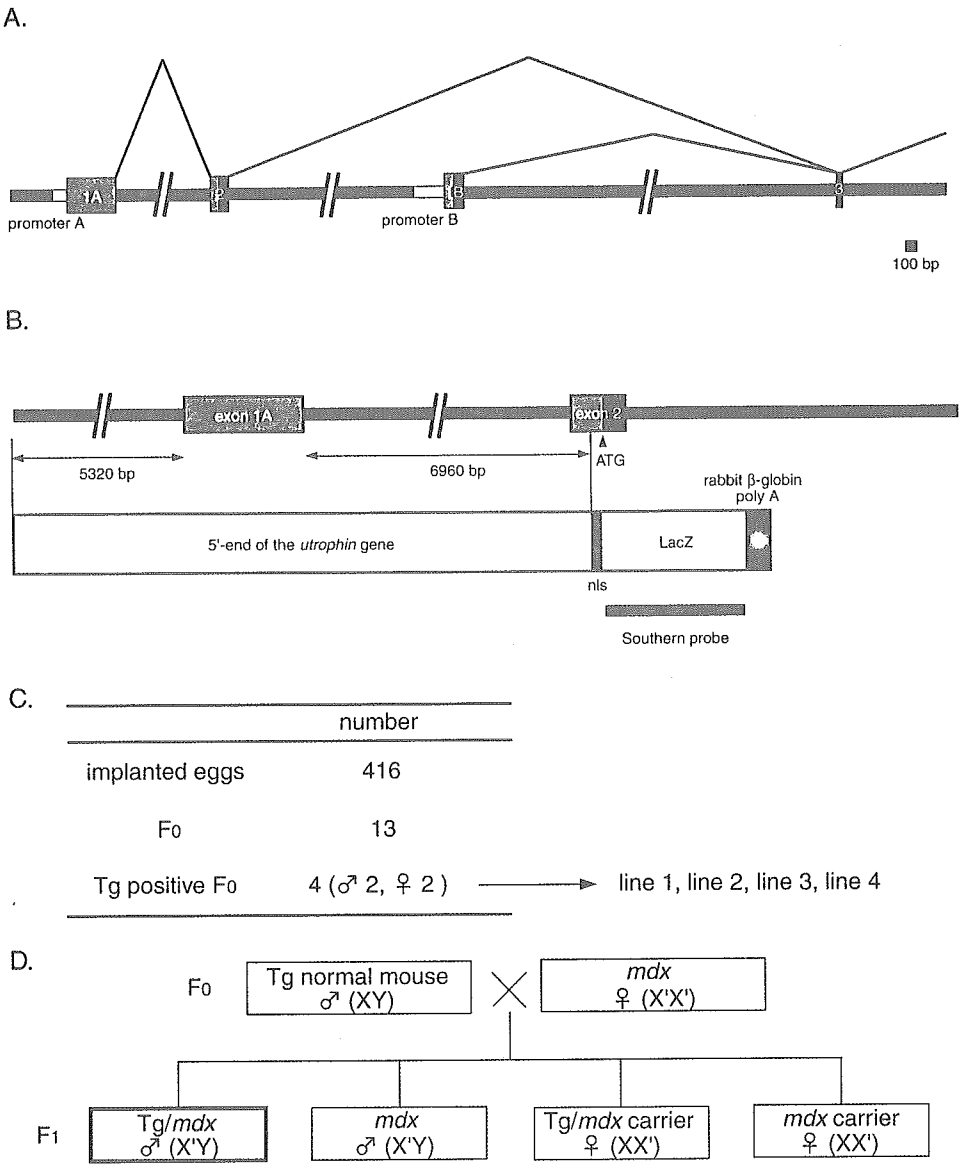

Figure 1. Generation of the A-utrophin promoter/nls LacZ transgenic mice. (A) Structure of the 5′ end of the *utrophin* gene. The *utrophin* gene is transcribed by two A and B promoters (white lines) that give rise to two transcripts, A-utrophin mRNA and B-utrophin mRNA, respectively. The two utrophin transcripts have different N-termini. Gray boxes indicate the 5′-UTR. Black boxes indicate the translated region of the exon. Scale bar indicates 100 bp. (B) Diagram of the transgene used in this study. The genomic fragment (12.4 kb), which contained the 5320-bp 5′-flanking region of the A-*utrophin* gene, exon 1A, and the first 59 bp of exon 2 UTR, was fused in-frame to a nls-tagged *LacZ* gene. Black bar indicates the Southern probe used to determine genotypes. (C) Summary of generation of transgenic mice. (D) Generation of transgenic *mdx* mice. Bold box indicates transgenic *mdx* male mice used in this study

probe, and hybridized with membranes at 65 °C overnight. The membranes were then washed extensively (2× SSPE, 0.1% SDS; 1× SSPE, 0.1% SDS; 0.1× SSPE, 0.1% SDS) at 65 °C and analyzed by BAS 2500 (Fuji Film, Japan).

Isolation of total RNA

Three-week-old Tg mice and wild-type littermates were sacrificed, and tissues were isolated and rapidly frozen in liquid nitrogen. Total RNA was isolated from frozen tissues using TRIzol reagent (Invitrogen Life Technologies, USA) according to the manufacturer's protocol. Finally, total RNA was treated with 1 U of RNase-free DNase I (Invitrogen Life Technologies) per microgram of RNA at room temperature for 15 min, and DNase I was inactivated by the addition of 25 mM EDTA (pH 8.0) and heating at 65 °C for 10 min.

Reverse transcription (RT)-PCR

RT was performed with 3.5 μg of total RNA using SuperScript II™ (Invitrogen Life Technologies) according to the manufacturer's protocol. PCR was performed using the *utrophin* exon 1A sense (5′-GGCGTTTCCAATCGGGTGTC-3′) and the *LacZ* gene antisense (5′-GCGGGCCTCTTCGCTATTAC-3′) primers for 35

cycles (denaturation at 95 °C for 1 min, annealing at 59 °C for 30 s, and extension at 72 °C for 1 min). As a control for the generation of PCR products due to residual contamination of genomic DNA, an equivalent amount of RNA that had not been treated with RT was also tested in parallel. The RT-PCR products of all samples were compared with the levels for a housekeeping gene, 18s rRNA, amplified with the following primer pair: sense primer (5′-TACCCTGGCGGTGGGATTAAC-3′) and anti-sense primer (5′-CGAGAGAAGACCACGCCAAC-3′). Amplification of A-utrophin was performed with the following primer pair: the *utrophin* gene exon 1A sense primer (5′-GGCGTTTCCAATCGGGTGTC-3′) and the *utrophin* gene exon 2 anti-sense primer (5′-CGTTCTGCCCATCATCAGGC-3′).

5′ RACE analysis

5′ RACE was carried out using the 5′ RACE system for rapid amplification of cDNA ENDs, V.2 kit (Invitrogen Life Technologies) following the manufacturer's protocol. Total RNA was reverse-transcribed using the *LacZ* gene-specific primer (GSP)-1 (5′-CGGATTGACCGTAATGGGATA-3′). The anchor-ligated cDNA was then PCR-amplified using the abridged anchor primer provided and the *LacZ* gene anti-sense primer, which was designed upstream of GSP-1, GSP-2 (5′-GCGGGCCTCTTCGCTATTAC-3′). In addition, the primary PCR product was amplified using the abridged universal amplification primer provided and the *nls* anti-sense primer, GSP-3 (5′-CGCTCATGATGCACGGTCTG-3′) designed upstream of GSP-2. PCR products were cloned into a pCR2.1 vector (Invitrogen Life Technologies) and sequenced using a Thermo Sequenase cycle sequencing kit (Amersham Biosciences).

Histochemical analysis

After Tg and wild-type mice had been sacrificed, cerebrum, cerebellum, submandibular gland, lung, kidney, liver, small intestine, colon, testis, pancreas, spleen, TA and soleus muscles, diaphragm, and heart were isolated and frozen in liquid nitrogen cooled isopentane. Cryosections (10 μm) from several tissues were stained with hematoxylin and eosin (H&E) and with 5-bromo-4-chloro-3-indolyl-β-D-galactopyranoside (X-Gal; Wako Chemicals, Japan) as described elsewhere [26].

Immunohistochemistry

Serial transverse cryosections (6 μm) from different tissues were placed on a slide, then dried and fixed in acetone for 6 min at −20 °C. We carried out immunohistochemical analysis with a rabbit polyclonal antibody against human utrophin (UT-2), which recognizes amino acid positions 1768–2078 [27]. The primary antibodies were detected with Alexa 488-labeled goat anti-rabbit IgG (Molecular Probes, USA). The nucleus was stained with TOTO-3 iodide (Molecular Probes). The NMJ was stained with Alexa 594-labeled α-bungarotoxin (α-BTX) (Molecular Probes). Signals were recorded photographically with a laser-scanning confocal imaging system (TCSSP™, Leica).

Cardiotoxin injection

To cause muscle degeneration, we injected 100 μl of cardiotoxin (CTX) of *Naja naja atra* venom (10 μM in saline, Wako Chemicals) into the right TA muscle of 5-week-old Tg mice with a 29-gauge needle. The concentration of CTX was determined according to a previous report [28]. CTX-injected Tg mice were sacrificed 1–7 days after CTX injection. The CTX-injected and contralateral non-injected TA muscles were isolated and frozen in liquid nitrogen cooled isopentane. Cryosections (10 μm) were stained with X-Gal. At the same time, serial cryosections (6 μm) were stained with UT-2 together with Alexa 594-labeled α-BTX. Total RNA was isolated from these frozen tissues.

Administration of rIL-6 to Tg/mdx mouse muscles

To investigate the effect of IL-6 on utrophin promoter A activation, we daily injected rIL-6 (800 ng in 6 μl of phosphate-buffered saline (PBS)/day) (R&D Systems, USA) for 5 days into the TA muscles of 2-week-old Tg/*mdx* mice. rIL-6-injected Tg/*mdx* mice were sacrificed 2 days after the final injection.

Results

Generation of four mouse lines with varying numbers of copies of the promoter A/nlsLacZ transgene

To investigate the utrophin promoter A activity, we first screened a 129Sv mouse genomic library and obtained a genome clone that contained the 5320-bp 5′-flanking region of the A-*utrophin* gene and exon 1A, intron 1, and exon 2. We then subcloned it into a Bluescript II vector. Subsequently, an nls-tagged *LacZ* gene was inserted downstream of the exon 2 UTR, as shown in Figure 1B. The nls was tagged to the *LacZ* gene to clarify the nuclei in which the utrophin promoter A was activated. Four transgenic F_0 'founder' mice were identified by Southern blotting using a *LacZ* probe, and four transgenic lines were established (Figure 1). The approximate number of transgene copies was determined by Southern blotting in all four lines (data not shown). Line 1 contained about 13 copies, lines 2 and 3 contained 5–6 copies, and line 4 contained 1 copy of the transgene.

mRNA levels of the transgene in several organs of Tg mice

The level of the transgene expression in several organs of Tg mice was determined by RT-PCR. Representative results from line 2 are shown in Figure 2. High levels of transgene mRNA expression were detected in liver, testis, colon, and submandibular gland. The signal was weakly detected in small intestine and lung, and an extremely low signal was detected in kidney, cerebrum, cerebellum, and TA muscle.

Determination of the 5′ end of β-gal mRNA

To investigate whether the transcription start site of the transgene corresponds to the authentic transcription start site of A-utrophin, we carried out 5′ RACE using total RNA isolated from testis of Tg mice (line 2). We obtained a single PCR product, indicative of a single transcription start site in testis (Figure 3). We sequenced the PCR product (543 bp) and confirmed the transcription start site of the transgene in testis, which was the same as that previously reported [16].

β-Gal expression in liver, testis, colon, submandibular gland, and small intestine of Tg mice

To identify the nuclei that express the transgene, cryosections were stained with X-Gal. At the same time, serial cryosections were stained with H&E or with UT-2, a polyclonal antibody against human utrophin [27] (Figure 4). UT-2 recognizes only the full-length form

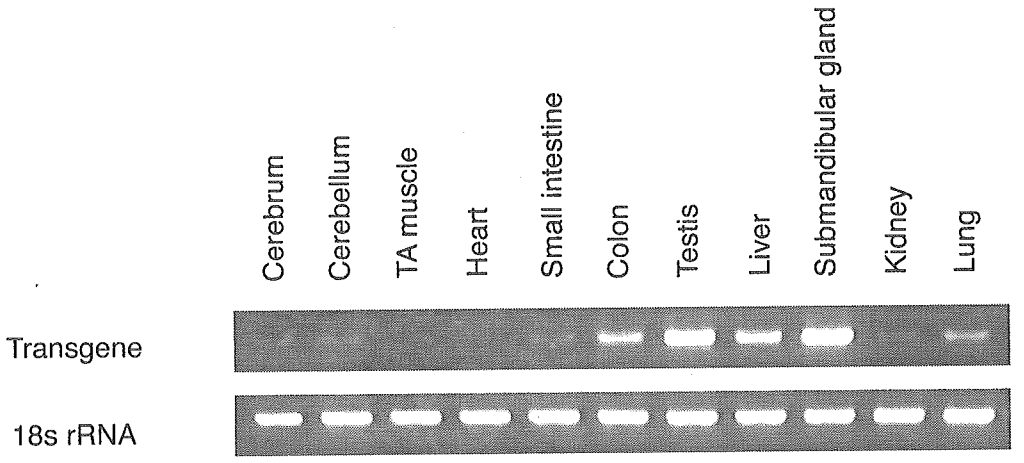

Figure 2. RT-PCR analysis of transgene mRNA from several tissues of transgenic mice. Total RNA was extracted from several tissues of 3-week-old line 2 Tg mice, and RT-PCR was performed with the transgene-specific primers described in Materials and methods. PCR products were electrophoresed on a 2% agarose gel. The expected size of the PCR product was 414 bp (transgene; *top*). As a control, 18s rRNA (297 bp; *bottom*) was co-amplified

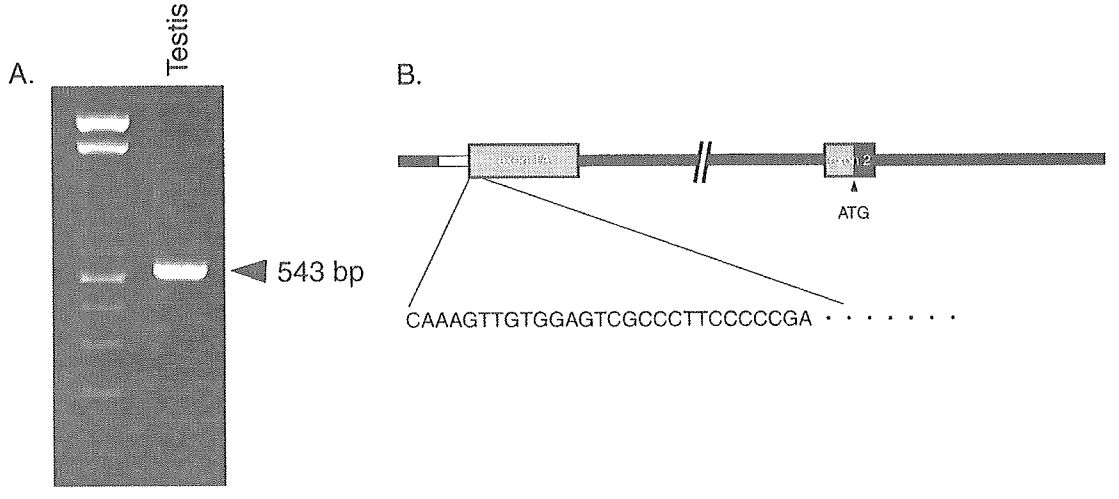

Figure 3. 5′ RACE analysis of transcription initiation sites. (A) 5′ RACE analysis with total RNA (1.5 μg) of the testis from 3-week-old line 2 Tg mice was performed using the gene-specific primers described in Materials and methods. The final PCR products were separated on a 2% agarose gel. (B) Sequencing products confirmed that the transgene was transcribed from the authentic initiation site of the utrophin A promoter (data not shown)

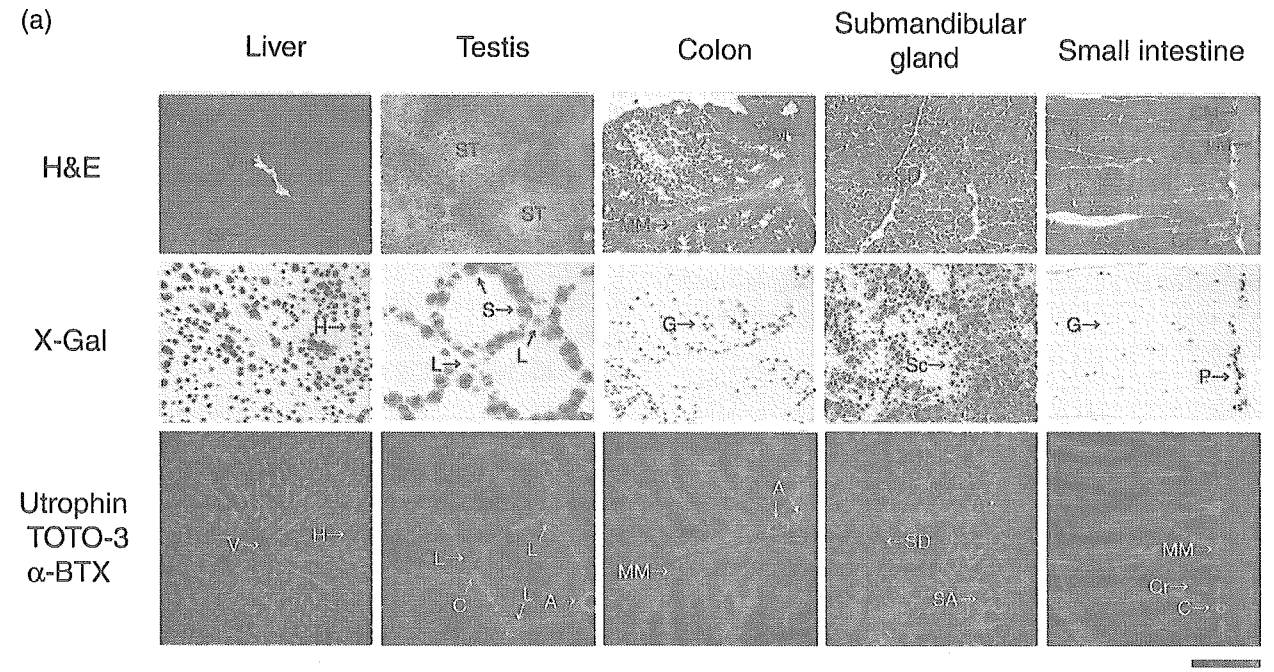

Figure 4. Histological and immunohistochemical analysis of transgenic mice. Cryosections (10 μm) were prepared from tissues (liver, testis, colon, submandibular gland, and small intestine (A), kidney and lung (B), cerebrum, cerebellum, heart, and TA muscle (C)) from 8-week-old line 2 Tg mice and stained with H&E (*top*) or X-Gal (*middle*). Serial 6 μm cryosections were stained with a polyclonal antibody against utrophin (UT-2; green). Nuclei were stained with TOTO-3 (blue). The NMJs were identified with α-BTX (red) (*bottom*). Shown are representative results obtained from line 2 Tg mice. Identical staining patterns were seen in all transgenic lines. V, terminal hepatic venule; Si, sinusoid; H, hepatocyte; ST, seminiferous tubule; L, Leydig cell; S, Sertoli cell; C, capillary; A, arteriole; MM, muscularis mucosa; CM, inner circular muscle layer; LM, outer longitudinal muscle layer; G, goblet cell; SD, striated duct; Sc, serous secretory cell; SA, serous acinus; Vi, villus; Cr, crypt; P, Paneth cell; T, cortical renal tubule; Gl, glomerulus; Al, alveolar cell; PV, pulmonary veinule; CP, choroid plexus; PM, pia mater; CC, cerebral cortex; N, neuron; ML, molecular layer; GL, granular layer; P, Purkinje cell; ID, intercalated disk; NMJ, neuromuscular junction. Bar, 100 μm

that includes both A-utrophin and B-utrophin [27]. We examined β-gal expression in all tissues in which A-utrophin has been reported to be expressed [20], and found that β-gal expression coincided well with endogenous A-utrophin expression in liver, testis, colon, submandibular gland, and small intestine.

In the liver, the nuclei of hepatocytes, but not sinusoid lining cells, were strongly stained with X-Gal, while endogenous utrophin protein was detected in the margins of hepatocytes along sinusoids and terminal hepatic venules.

In the testis, β-gal activity was found in Sertoli cells in the basal compartment of the seminiferous tubules, but not in the adluminal compartment, and in Leydig cells in the interstitial supporting tissues between the seminiferous tubules. Consistent with this observation, endogenous utrophin signals were found along the basement membrane of the seminiferous tubules and Leydig cells.

In the colon, β-gal-positive nuclei were found in goblet cells in large intestinal glands. Endogenous utrophin signals were found along the basement membrane of large intestinal glands and muscularis mucosa.

In the submandibular gland, the nuclei of both serous and mucous secretory cells were clearly stained with X-Gal. The striated duct epithelia lacked the β-gal signal. Endogenous utrophin was detected along the basement

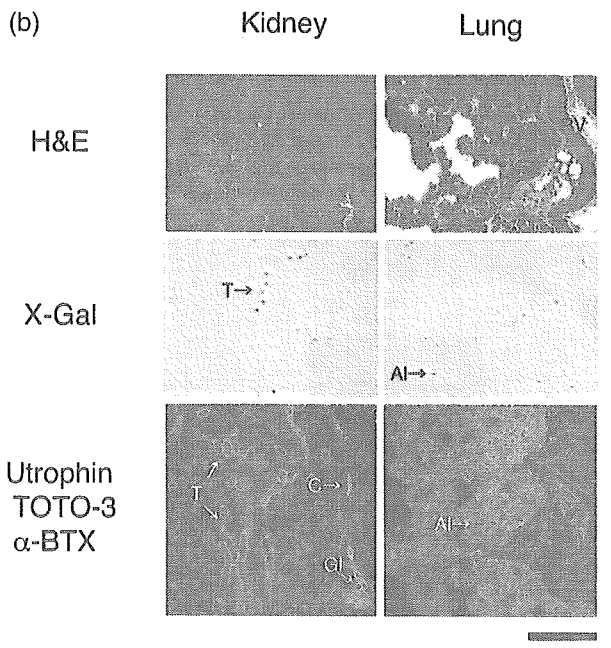

Figure 4. (*Continued*)

membrane of serous and mucous acini, but not of striated ducts.

In the small intestine, β-gal-positive nuclei were found in goblet cells and epithelia of the bases of villi and crypts.

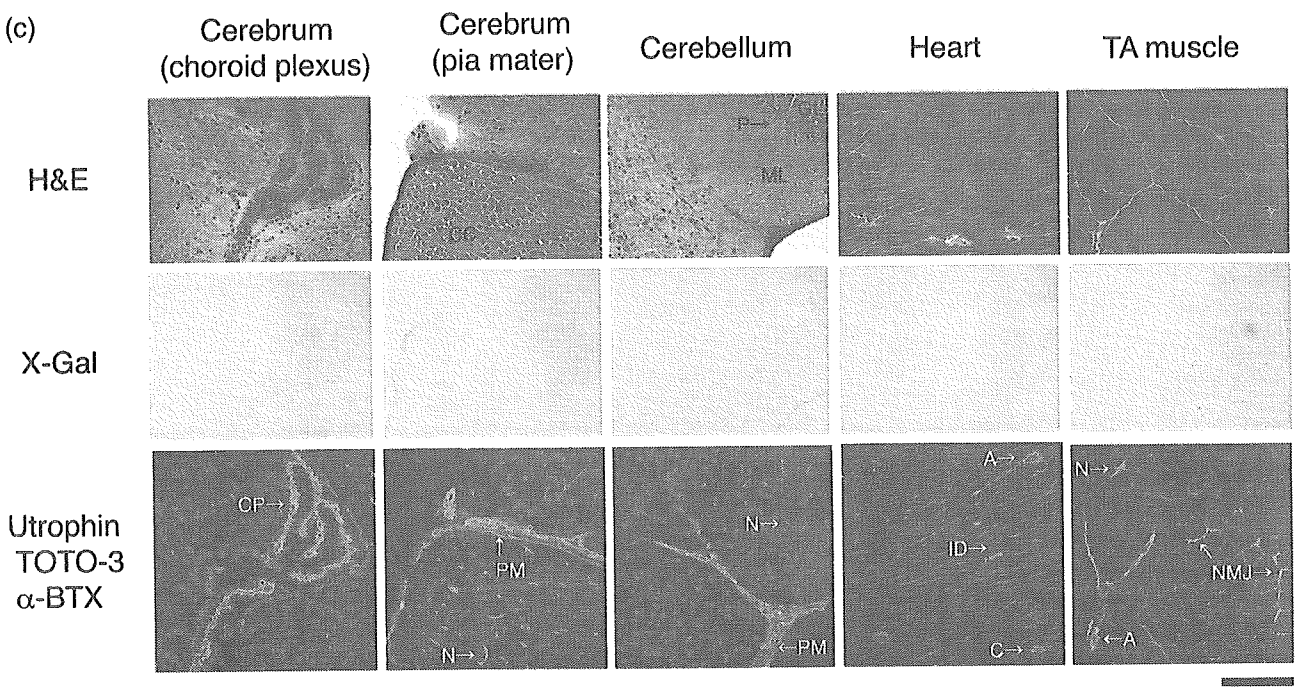

Figure 4. ***(Continued)***

β-Gal signals were stronger in a subset of cells, and their characteristic distribution suggests that these cells were Paneth cells. Endogenous utrophin signals were found along the basement membrane of villi and crypts and in muscularis mucosa.

In the kidney, β-gal-positive nuclei were found in the epithelia of cortical renal tubules, but not in glomeruli. It is not clear whether β-gal-positive nuclei were present in proximal convoluted tubules, distal convoluted tubules, collecting tubules, or collecting ducts. Endogenous utrophin was found along the basement membrane of cortical renal tubules, collecting ducts of the renal medulla and Bowman's capsules, and in glomerular capillaries.

In the lung, β-gal-positive nuclei were found in alveoli, but not in terminal bronchiole epithelia. It is not clear whether β-gal-positive nuclei were present in type I or type II pneumocytes. Endogenous utrophin was found in alveolar cells and terminal bronchiole epithelia. Thus, in these tissues, endogenous utrophin protein seems to localize at the plasma membranes of cells adjacent to the basement membranes.

Inconsistent results of *LacZ* expression among the four transgenic lines

In the pancreas, β-gal-positive nuclei were clearly found in exocrine cells of lines 1 and 2, but not at all in lines 3 and 4 (data not shown). Because of this inconsistency of β-gal expression patterns among the four Tg lines, we could not determine the relationship between β-gal and endogenous utrophin expression in pancreas.

β-Gal-positive nuclei were ubiquitously found in the cerebrum of line 1, but not in other lines (Table 1). The A-utrophin protein has been shown to be expressed in the pia mater and choroid plexus of the brain [20]. Nevertheless, our results indicate that the A-utrophin promoter was not active in the pia mater and choroid plexus in our Tg mice (Figure 4C).

In the cerebellum, β-gal-positive nuclei were found in granular cells of lines 1 and 3, but not at all in lines 2 and 4 (Figure 4C, Table 1). The A-utrophin protein has been shown to be expressed in the pia mater of the cerebellum [20]. Nevertheless, our results indicate that the A-utrophin promoter was not active in the pia mater of the cerebellum in our Tg mice (Figure 4C). We speculate that this discrepancy is due to the positional effects of the transgene integration into the mouse genome.

In the spleen, β-gal-positive nuclei were not found in any of the four lines, although endogenous utrophin was found in endothelial cells of venous sinuses in red pulp (data not shown). It seems that β-gal expression was not detected in spleen of our Tg lines because B-utrophin was observed in endothelia of blood vessels [20].

β-Gal-positive nuclei were not found in cardiac, skeletal, or vascular smooth muscle

A previous study using antibodies specific to A- and B-utrophins showed that, in skeletal muscle, A-utrophin is expressed in the NMJ, peripheral nerves, and larger blood vessels [20]. However, we detected β-gal expression in neither the NMJ nor peripheral nerves of Tg skeletal muscles. As expected, β-gal expression was not found in blood vessels of Tg mouse tissues, where B-utrophin has been reported to be expressed. Unexpectedly, we did

Table 1. Summary of β-gal expression in four transgenic lines. Tg mice (lines 1–4) were sacrificed at 3 weeks old and 8 weeks old and β-gal expression in several tissues was examined. No β-gal-positive nuclei were found in non-transgenic littermates. β-Gal expression level is shown as follows: –, none; ±, trace; +, weak; ++, moderate; +++, strong

	Young (3–5w)				Adult (8–18w)			
	line 1	line 2	line 3	line 4	line 1	line 2	line 3	line 4
Cerebrum	++	–	–	–	++	–	–	–
Cerebellum	+	–	+	–	++	–	+	–
Heart	–	–	–	–	–	–	–	–
TA muscle	–	–	–	–	–	–	–	–
Soleus muscle	–	–	–	–	–	–	–	–
Diaphragm	–	–	–	–	–	–	–	–
Arteriole	–	–	–	–	–	–	–	–
Small intestine	+	+	+	–	+	+	–	–
Colon	+	++	++	++	++	++	+	+
Testis	+++	+++	++	–	+++	+++	++	–
Liver	++	++	±	±	++	+++	±	±
Submandibular gland	+++	+++	++	–	+++	+++	++	–
Kidney	+	±	±	±	±	±	–	–
Lung	++	+	–		+	+	–	–
Pancreas	++	+	–	–	++	+	–	–
Spleen	–	–	–	–	–	–	–	–

Table 2. Cells that express β-gal in transgenic mice and comparison with endogenous utrophin expression. Examined tissues were categorized into three groups. Group I: β-gal expression and endogenous utrophin expression coincide well. Group II: β-gal expression partially recapitulates endogenous utrophin expression. Group III: β-gal expression was not detected in spite of endogenous utrophin expression. The localization of endogenous utrophin is based on this study and previous studies [20]. BM, basement membrane; N.D., not detected

	Tissue	Endogenous utrophin	β-Gal expression
I	Liver	Surface of hepatocyte (space of Disse)	hepatocyte
	Testis	BM of seminiferous tubule	Sertoli cell
		Leydig cell	Leydig cell
	Colon	BM of large intestinal gland	goblet cell
		muscularis mucosa	N.D.
	Submandibular gland	BM of serous & mucous acinus	serous & mucous secretory cell
	Small intestine	BM of villus & crypt	Paneth cell, goblet cell
		muscularis mucosa	N.D.
II	Kidney	BM of cortical renal tubule	epithelial cell of cortical renal tubule
		BM of collecting duct in renal medulla	
		glomerulus	N.D.
	Lung	alveolus	alveolar cell
		terminal bronchiole epithelium	N.D.
III	Cerebrum	choroid plexus	N.D.
		pia mater	
	Cerebellum	pia mater	N.D.
	Heart	intercalated disk	N.D.
		T tubule	
	Skeletal muscle	neuromuscular junction	N.D.
		myotendinous junction	
		regenerating muscle fiber	
	Blood vessel	vascular smooth muscle	N.D.
		endothelium	
		capillary	
	Spleen	endothelial cell of venous sinus in red pulp	N.D.

not detect β-gal expression signals in Tg vascular smooth muscle. Furthermore, cardiac muscle in transgenic mice showed no β-gal-positive nuclei (Figure 4C).

β-Gal expression in the four Tg lines is summarized in Table 1. Table 2 is a comparison between β-gal expression and immunohistochemical detection of endogenous utrophin in the utrophin promoter A-*LacZ* transgenic mice. Group I consists of the tissues in which the pattern of β-gal expression corresponded well to that of endogenous utrophin. Group II includes the tissues in which β-gal-positive nuclei were found in only a few subsets of cells expressing endogenous utrophin. Group III contains the tissues in which A-utrophin is reported to be expressed [20], but β-gal expression was not detected at all.

Regenerating and *mdx* skeletal muscles show no expression of transgene

Utrophin is up-regulated in *mdx* muscle. To analyze the β-gal expression in Tg/*mdx* muscle, we mated Tg F_1 male

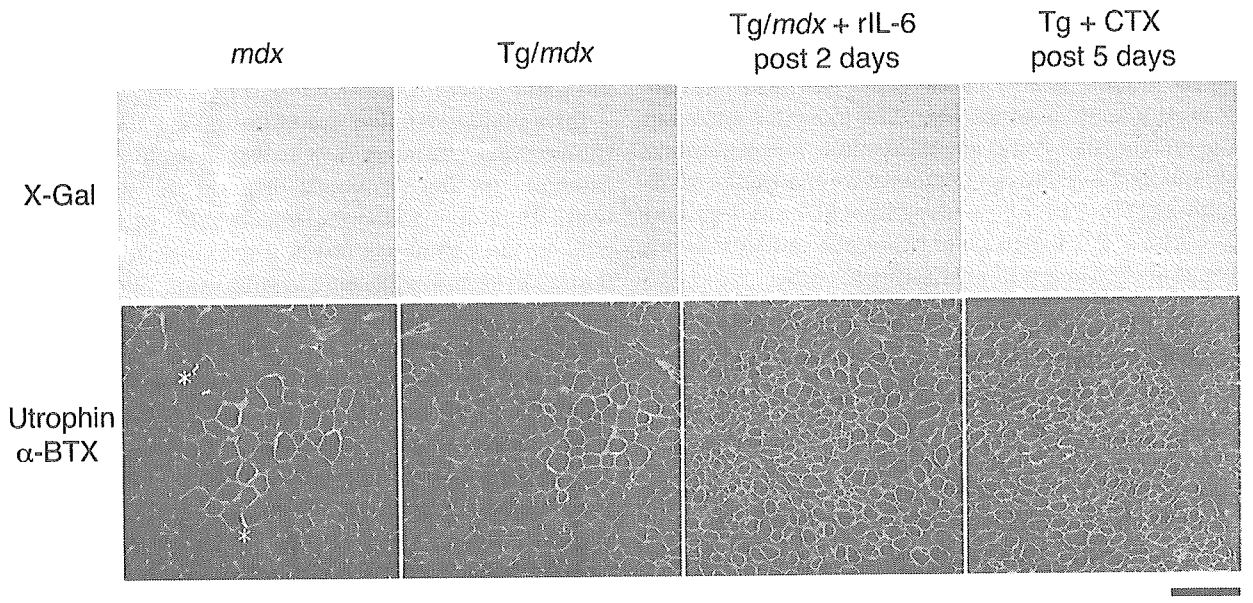

Figure 5. Effects of recombinant IL-6 and CTX injection into TA muscle of transgenic mice on transgene expression (β-gal). Cryosections of TA muscle from *mdx* mice, Tg *mdx* male mice (Tg/*mdx*), CTX-injected Tg TA muscle (Tg + CTX), and rIL-6-injected Tg *mdx* TA muscle (Tg/*mdx* + rIL-6) were stained with X-Gal (*top*) or stained with a polyclonal antibody against utrophin (UT-2) (green) and Alexa 594-labeled α-BTX (red) (*bottom*). rIL-6-injected Tg/*mdx* TA muscles were obtained 2 days after the final injection of rIL-6, and CTX-injected Tg TA muscles were obtained 5 days after CTX injection. * indicates NMJ. Bar, 100 μm

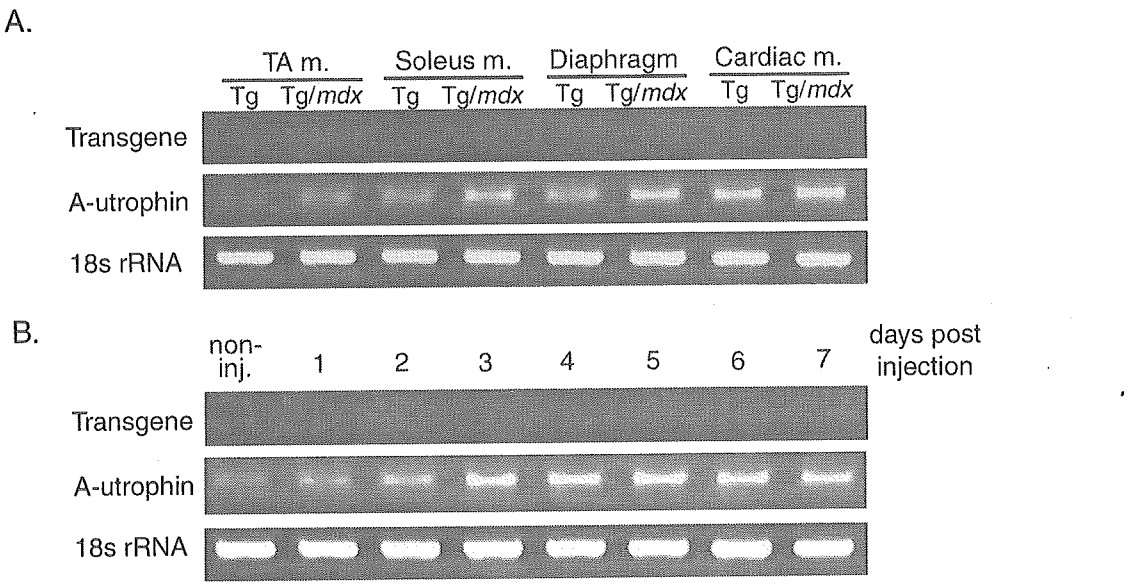

Figure 6. Effects of muscle regeneration on expression of transgene mRNA. Total RNA was extracted from TA muscle, soleus muscle, diaphragm, and cardiac muscle of 4-week-old Tg and Tg/*mdx* mice (A), and from CTX-injected 5-week-old Tg TA muscles at the indicated days after the injection (B). RT-PCR was performed with transgene-specific primers described in Materials and methods. PCR products were electrophoresed on 2% agarose gel. The expected size of PCR products was 414 bp (transgene; *top*) and 309 bp (A-utrophin; *middle*). As a control, 18s rRNA (297 bp; *bottom*) was co-amplified

mice of line 2 with *mdx* female mice (Figure 1D). Utrophin protein was overexpressed along the sarcolemma of *mdx* muscle fibers, but all myonuclei were negative for β-gal staining (Figure 5). Next, we investigated the mRNA levels of A-utrophin and transgene by RT-PCR. To this end, A-utrophin mRNA was elevated in TA muscle, soleus muscle, diaphragm, and cardiac muscle of Tg/*mdx* mice, but transgene mRNA was not detected in these muscles (Figure 6A). In addition, there was no difference in β-gal expression in various tissues other than muscle between Tg/*mdx* male mice and parental C57BL/6J-Tg mice (data not shown).

Utrophin is up-regulated in regenerating muscle. Recently, Galvagni *et al.* reported that the transcription of A-utrophin was elevated in regenerating muscle [19]. Therefore, we next injected CTX into TA muscle of line 2 Tg mice to damage muscle fibers, and analyzed β-gal expression during muscle regeneration (Figure 5).

Figure 5 shows a section of transgenic skeletal muscle isolated 5 days after CTX injection, chosen because the utrophin protein signal was detected the most strongly in it of all tissues collected after CTX injection. Utrophin was overexpressed along the sarcolemma of regenerating small muscle fibers, but all myonuclei were negative for β-gal staining. Furthermore, A-utrophin mRNA was elevated 3 days after CTX injection, but transgene mRNA was not detected in CTX-injected muscle (Figure 6B).

Administration of rIL-6 did not induce the expression of the transgene in skeletal muscle

We have previously reported that rIL-6 induced overexpression of endogenous utrophin in *mdx* skeletal muscle [24]. Subsequently, we found that rIL-6 elevated mainly A-utrophin mRNA (Itoh *et al.*, unpublished data). Therefore, we injected rIL-6 into the TA muscles of Tg/*mdx* mice daily for 5 days and analyzed the effect of rIL-6 on the transgene expression (Figure 5). Without doubt, rIL-6 induced overexpression of utrophin in Tg/*mdx* muscles, but not expression of the transgene (Figure 5). Furthermore, A-utrophin mRNA was up-regulated 2 days after the final injection, but transgene mRNA was not detected (data not shown).

Discussion

Previous transgenic studies showed that forced expression of utrophin at the sarcolemma of *mdx* muscle dramatically improved dystrophic phenotypes [11–13]. Furthermore, an adenovirally induced *utrophin* gene ameliorated the dystrophic changes in *mdx* mice [14]. On the other hand, we have previously reported that adenovirus vector-mediated expression of β-gal up-regulated endogenous utrophin at the sarcolemma in *mdx* muscle, where β-gal-positive muscle fibers were protected from the degeneration process [15]. Thus, up-regulation of utrophin stabilizes dystrophin-deficient muscle membrane and protects muscle fibers from degeneration caused by mechanical stress.

There are two full-length transcripts: A-utrophin and B-utrophin [16,17]. A-Utrophin localizes to the NMJ and in peripheral nerves [20]. The upstream promoter A is CpG-rich, TATA-less, and contains a consensus N-box, which is critical for synaptic expression of utrophin. In contrast, B-utrophin is observed in endothelial capillaries and vessels [20]. Further, A-utrophin, but not B-utrophin, is up-regulated in regenerating muscle fibers [19] or in *mdx* muscle fibers [20]. Therefore, we first examined promoter A activity using transgenic techniques. The *LacZ* gene was tagged by nls to clarify the nuclei in which promoter A is active. Contrary to our expectation, analysis of both transcripts for the transgene and β-gal staining showed that the 5320-bp 5′-flanking region of the A-*utrophin* gene is highly and constantly active in liver, testis, colon, submandibular gland, and small intestine, slightly active in kidney and lung, but not at all in striated muscles.

Intriguingly, detailed examination at the cellular level showed that promoter A is active in secretory cells. For example, in the Tg mouse liver, β-gal-positive nuclei were found in hepatocytes, which synthesize and secrete bile. In the Tg mouse testis, β-gal-positive nuclei were found in Sertoli cells and Leydig cells. Sertoli cells of the fetal testis produce and secrete Mullerian-inhibiting substance (MIS), which suppresses the development of the reproductive tract and results in regression of the Mullerian duct in the female. MIS is also produced in the adult gonads and plays a role in maintaining testosterone homeostasis [29]. Leydig cells synthesize and secrete testosterone, which induces male secondary sexual characteristics. In the Tg mouse colon, β-gal-positive nuclei were found in goblet cells, which produce mucin. In the submandibular gland, nuclei of serous or mucous secretory cells, which secrete saliva, were clearly stained with X-Gal, although the Tg mouse striated duct epithelia, which secrete lysozyme and IgA, lacked β-gal expression. In the Tg mouse small intestine, β-gal-positive nuclei were found in goblet cells and Paneth cells. Goblet cells secrete mucus, and Paneth cells secrete microbicidal α-defensins when exposed to bacteria or bacterial antigens [30]. Previous studies showed that utrophin is found at high levels in secretory tissues including pituitary, thyroid, adrenal glands, and choroid plexus epithelia, which secrete glucocorticoid hormones, the iodine-containing hormones tri-iodothyronine and thyroxine, steroid and catecholamine hormones, and cerebrospinal fluid, respectively [31,32]. We detected A-utrophin expression in the secretory cells of our Tg mice. We speculate that utrophin may have other unknown functions as well as supporting secretory cells.

In the Tg mouse kidney, endogenous utrophin was expressed in glomerular tufts, cortical renal tubules, and collecting ducts in the renal medulla, and A-utrophin protein has been shown to be expressed in glomerular tufts and tubules of the renal cortex [20]. However, β-gal signals were found in only a few epithelia of cortical renal tubules. On the other hand, endogenous utrophin signals were found along the basement membrane of cortical renal tubules, possibly assembling the DAP complex at the plasma membrane and interacting with laminin in the basement membrane. The reason β-gal-positive nuclei were not found in glomeruli is unknown. In the Tg mouse lung, a small number of β-gal-positive nuclei were found in a few type I or type II pneumocytes. The reason for this discrepancy is unclear.

In the cerebrum and the cerebellum of Tg mice, transgene mRNA was detected at extremely low levels, while β-gal-positive nuclei were not detected at all in the choroid plexus and pia mater. In these tissues, the transcriptional level was also low, and the stability of transgene mRNA may be lower than the transcriptional level, as in skeletal muscle.

In this study, unexpectedly, we detected extremely low levels of transgene mRNA in skeletal muscle and no β-gal staining in myonuclei even in the vicinity of the NMJs. Likewise, the expression of the transgene was not observed in regenerating muscle of the utrophin promoter A/*LacZ* transgenic mice. Further, we previously reported that IL-6 induced overexpression of utrophin in neonatal *mdx* muscle [24]. However, the expression of β-gal was not observed in rIL-6-injected Tg/*mdx* muscle. Briefly, the promoter of the A-*utrophin* gene is not active in cardiac and skeletal muscle, and there are several possibilities for a regulatory mechanism of A-utrophin expression in skeletal and cardiac muscle. First, the transgene construct used in this study contained the 5′-flanking region (5320 bp) of the A-*utrophin* gene, but lacked the intronic enhancer (downstream utrophin enhancer, DUE) within the second intron, which has recently been reported [18]. Therefore, it is reasonable to speculate that the intronic enhancer is indispensable for the expression of utrophin in both skeletal muscle and cardiac muscle. Second, the 5320 bp of the 5′-flanking region or first intron might contain a silencer region for the expression of A-utrophin in skeletal and cardiac muscle, since Galvagni *et al.* reported that *LacZ* expression was detected in muscle cell transfected with the promoter alone [19]. Third, important roles for the 3′-UTR of utrophin mRNA in stabilization have been suggested, and two RNA-binding proteins have been reported [22]. For example, Gramolini *et al.* reported ~42- kDa and 90-kDa proteins that bind utrophin 3′-UTR and are expressed more abundantly in extensor digitorum longus muscles than in soleus muscles. Hence, higher levels of utrophin mRNA in soleus muscles suggest that these proteins destabilize utrophin mRNA [22]. Furthermore, Gramolini *et al.* reported that the utrophin 3′-UTR is responsible for targeting utrophin mRNA to cytoskeletal-bound polysomes, binding actin, and controlling transcript stability [23]. We previously reported that adenovirus vector-mediated gene transfer into skeletal muscle evoked robust expression of endogenous utrophin via immune response [15], in which both A-utrophin and B-utrophin mRNA levels were continuously elevated (Itoh *et al.*, unpublished data). These results suggest that utrophin overexpression is induced by one or more inflammatory cytokines, and most of the effects seem to be due to post-transcriptional regulation. These observations and our results suggest that the expression of utrophin in skeletal muscle might be regulated at the post-transcriptional level via 3′-UTR. Finally, it is also important to note that the utrophin protein seems to be relatively stable at the sarcolemma in skeletal muscle [22]. Once the utrophin protein forms the dystrophin–glycoprotein complex at the sarcolemma, it might be extremely stable in muscle fibers compared with β-gal.

In summary, we showed here that the 5-kb flanking region of the A-*utrophin* gene containing the A-utrophin core promoter drives high levels of A-utrophin transcription in liver, testis, colon, submandibular gland, and small intestine, but not in skeletal and cardiac muscle, indicating that A-utrophin expression in striated muscle is greatly dependent on other regulatory elements.

Acknowledgements

We thank Dr. Hirata and Dr. Yokota for technical instructions. We also thank S. Masuda and A. Fukase for technical assistance, and colleagues in our laboratory for useful discussion and suggestions on this work. This work is supported by Grants-in-Aid for Center of Excellence (COE), Research on Nervous and Mental Disorders (10B-1, 13B-1), and Health Science Research Grants for Research on the Human Genome and Gene Therapy (H10-genome-015, H13-genome-001), for Research on Brain Science (H12-Brain-028, H15-Brain-021) from the Ministry of Health, Labor and Welfare, Grants-in Aids for Scientific Research (10 557 065, 11 470 153, 11 170 264, 14 657 158 and 15 390 281) from the Ministry of Education, Culture, Sports, Science and Technology, and a Research Grant from the Human Frontier Science Project.

References

1. Koenig M, Hoffman EP, Bertelson CJ, *et al.* Complete cloning of the Duchenne muscular dystrophy (DMD) cDNA and preliminary genomic organization of the DMD gene in normal and affected individuals. *Cell* 1987; **50**: 509–517.
2. Ahn AH, Kunkel LM. The structural and functional diversity of dystrophin. *Nat Genet* 1993; **3**: 283–291.
3. Tinsley JM, Blake DJ, Zuellig RA, *et al.* Increasing complexity of the dystrophin-associated protein complex. *Proc Natl Acad Sci U S A* 1994; **91**: 8307–8313.
4. Campbell KP. Three muscular dystrophies: loss of cytoskeleton-extracellular matrix linkage. *Cell* 1995; **80**: 675–679.
5. Ozawa E, Yoshida M, Suzuki A, *et al.* Dystrophin-associated proteins in muscular dystrophy. *Hum Mol Genet* 1995; **4**: 1711–1716.
6. Pearce M, Blake DJ, Tinsley JM, *et al.* The utrophin and dystrophin genes share similarities in genomic structure. *Hum Mol Genet* 1993; **2**: 1765–1772.
7. Grady RM, Teng H, Nichol MC, *et al.* Skeletal and cardiac myopathies in mice lacking utrophin and dystrophin: a model for Duchenne muscular dystrophy. *Cell* 1997; **90**: 729–738.
8. Khurana TS, Watkins SC, Chafey P, *et al.* Immunolocalization and developmental expression of dystrophin related protein in skeletal muscle. *Neuromuscul Disord* 1991; **1**: 185–194.
9. Ohlendieck K, Ervasti JM, Matsumura K, *et al.* Dystrophin-related protein is localized to neuromuscular junctions of adult skeletal muscle. *Neuron* 1991; **7**: 499–508.
10. Wilson LA, Cooper BJ, Dux L, *et al.* Expression of utrophin (dystrophin-related protein) during regeneration and maturation of skeletal muscle in canine X-linked muscular dystrophy. *Neuropathol Appl Neurobiol* 1994; **20**: 359–367.
11. Tinsley JM, Potter AC, Phelps SR, *et al.* Amelioration of the dystrophic phenotype of mdx mice using a truncated utrophin transgene. *Nature* 1996; **384**: 349–353.
12. Deconinck N, Tinsley JM, De Backer F, *et al.* Expression of truncated utrophin leads to major functional improvements in dystrophin-deficient muscles of mice. *Nat Med* 1997; **3**: 1216–1221.
13. Tinsley JM, Deconinck N, Fisher R, *et al.* Expression of full-length utrophin prevents muscular dystrophy in mdx mice. *Nat Med* 1998; **4**: 1441–1444.
14. Gilbert R, Nalbantoglu J, Petrof BJ, *et al.* Adenovirus-mediated utrophin gene transfer mitigates the dystrophic phenotype of mdx mouse muscles. *Hum Gene Ther* 1999; **10**: 1299–1310.
15. Yamamoto K, Yuasa K, Miyagoe Y, *et al.* Immune response to adenovirus-delivered antigens upregulates utrophin and results in mitigation of muscle pathology in mdx mice. *Hum Gene Ther* 2000; **11**: 669–680.
16. Dennis CL, Tinsley JM, Deconinck AE, *et al.* Molecular and functional analysis of the utrophin promoter. *Nucleic Acids Res* 1996; **24**: 1646–1652.

17. Burton EA, Tinsley JM, Holzfeind PJ, *et al.* A second promoter provides an alternative target for therapeutic up-regulation of utrophin in Duchenne muscular dystrophy. *Proc Natl Acad Sci U S A* 1999; **96**: 14025–14030.
18. Galvagni F, Oliviero S. Utrophin transcription is activated by an intronic enhancer. *J Biol Chem* 2000; **275**: 3168–3172.
19. Galvagni F, Cantini M, Oliviero S. The utrophin gene is transcriptionally up-regulated in regenerating muscle. *J Biol Chem* 2002; **277**: 19106–19113.
20. Weir AP, Burton EA, Harrod G, *et al.* A- and B-utrophin have different expression patterns and are differentially up-regulated in mdx muscle. *J Biol Chem* 2002; **277**: 45285–45290.
21. Jimenez-Mallebrera C, Davies KE, Putt W, *et al.* A study of short utrophin isoforms in mice deficient for full-length utrophin. *Mamm Genome* 2003; **14**: 47–60.
22. Gramolini AO, Belanger G, Thompson JM, *et al.* Increased expression of utrophin in a slow vs. a fast muscle involves posttranscriptional events. *Am J Physiol Cell Physiol* 2001; **281**: C1300–C1309.
23. Gramolini AO, Belanger G, Jasmin BJ. Distinct regions in the 3′ untranslated region are responsible for targeting and stabilizing utrophin transcripts in skeletal muscle cells. *J Cell Biol* 2001; **154**: 1173–1183.
24. Fujimori K, Itoh Y, Yamamoto K, *et al.* Interleukin-6 induces overexpression of the sarcolemmal utrophin in neonatal mdx skeletal muscle. *Hum Gene Ther* 2002; **13**: 509–518.
25. Kalderon D, Roberts BL, Richardson WD, *et al.* A short amino acid sequence able to specify nuclear location. *Cell* 1984; **39**: 499–509.
26. Ishii A, Hagiwara Y, Saito Y, *et al.* Effective adenovirus-mediated gene expression in adult murine skeletal muscle. *Muscle Nerve* 1999; **22**: 592–599.
27. Imamura M, Ozawa E. Differential expression of dystrophin isoforms and utrophin during dibutyryl-cAMP-induced morphological differentiation of rat brain astrocytes. *Proc Natl Acad Sci U S A* 1998; **95**: 6139–6144.
28. Couteaux R, Mira JC, d'Albis A. Regeneration of muscles after cardiotoxin injury. I. Cytological aspects. *Biol Cell* 1988; **62**: 171–182.
29. Teixeira J, Fynn-Thompson E, Payne AH, *et al.* Mullerian-inhibiting substance regulates androgen synthesis at the transcriptional level. *Endocrinology* 1999; **140**: 4732–4738.
30. Ayabe T, Satchell DP, Wilson CL, *et al.* Secretion of microbicidal alpha-defensins by intestinal Paneth cells in response to bacteria. *Nat Immunol* 2000; **1**: 113–118.
31. Schofield J, Houzelstein D, Davies K, *et al.* Expression of the dystrophin-related protein (utrophin) gene during mouse embryogenesis. *Dev Dyn* 1993; **198**: 254–264.
32. Knuesel I, Bornhauser BC, Zuellig RA, *et al.* Differential expression of utrophin and dystrophin in CNS neurons: an in situ hybridization and immunohistochemical study. *J Comp Neurol* 2000; **422**: 594–611.

doi:10.1016/j.ymthe.2004.07.025

ARTICLE

AAV Vector-Mediated Microdystrophin Expression in a Relatively Small Percentage of *mdx* Myofibers Improved the *mdx* Phenotype

Madoka Yoshimura,[1,2] Miki Sakamoto,[1] Madoka Ikemoto,[1] Yasushi Mochizuki,[1] Katsutoshi Yuasa,[1] Yuko Miyagoe-Suzuki,[1] and Shin'ichi Takeda[1,*]

[1]*Department of Molecular Therapy, National Institute of Neuroscience, National Center of Neurology and Psychiatry, 4-1-1 Ogawa-higashi, Kodaira, Tokyo 187-8502, Japan*
[2]*Department of Neurology, Division of Neuroscience, Graduate School of Medicine, University of Tokyo, Hongo 7-3-1, Tokyo 113-8655, Japan*

**To whom correspondence and reprint requests should be addressed. Fax: +81 42 346 1750. E-mail: takeda@ncnp.go.jp.*

Available online 19 August 2004

Duchenne muscular dystrophy (DMD) is a lethal disorder of skeletal muscle caused by mutations in the *dystrophin* gene. Adeno-associated virus (AAV) vector-mediated gene therapy is a promising approach to the disease. Although a rod-truncated microdystrophin gene has been proven to ameliorate dystrophic phenotypes, the level of microdystrophin expression required for effective gene therapy by an AAV vector has not been determined yet. Here, we constructed a recombinant AAV type 2 vector, AAV2-MCKΔCS1, expressing microdystrophin (ΔCS1) under the control of a muscle-specific MCK promoter and injected it into TA muscles of 10-day-old and 5-week-old *mdx* mice. AAV2-MCKΔCS1-mediated gene transfer into 5-week-old *mdx* muscle resulted in extensive and long-term expression of microdystrophin and significantly improved force generation. Interestingly, 10-day-old injected muscle expressed microdystrophin in a limited number of myofibers but showed hypertrophy of microdystrophin-positive muscle fibers and considerable recovery of contractile force. Thus, we concluded that AAV2-MCKΔCS1 could be a powerful tool for gene therapy of DMD.

Key Words: Duchenne muscular dystrophy, gene therapy, adeno-associated virus vector, dystrophin, microdystrophin, skeletal muscle, *mdx* mouse, hypertrophy

INTRODUCTION

Duchenne muscular dystrophy (DMD) is an X-linked, lethal disorder of skeletal muscle caused by mutations in the *dystrophin* gene. There is no effective treatment for the disease at present, although gene therapy could be an attractive approach to the disease.

Several methods of gene transfer have been tried for the treatment of dystrophin-deficient muscular dystrophy: naked plasmid injection [1], full-length dystrophin cDNA transfer via a gutted adenovirus vector [2,3], forced splicing using oligonucleotides [4], and gene repair by a chimeric RNA/DNA oligonucleotide [5]. Among several gene transfer methods, an adeno-associated virus (AAV) vector-mediated gene transfer is one of the most promising approaches to DMD because AAV vectors have been shown to evoke minimal immune responses and mediate long-term transgene expression in skeletal muscle [6–8]. Since the capacity of an AAV vector to incorporate an exogenous gene is limited to 4.9 kb, several groups have attempted to truncate the 14-kb dystrophin cDNA to obtain functional microdystrophins to be inserted into AAV vectors [9–13]. We previously constructed three rod-truncated microdystrophins and generated transgenic *mdx* mice expressing these microdystrophins. Among the three microdystrophins tested, only the 4.9-kb microdystrophin CS1 completely prevented muscle degeneration of dystrophin-deficient *mdx* mice [14]. Based on this result, we generated an AAV vector carrying ΔCS1 microdystrophin cDNA, a modified version of CS1 cDNA, and injected the vectors (designated AAV2-MCKΔCS1) directly into both 10-day-old and 5-week-old *mdx* muscles. In this study, we demonstrate that AAV vector-injected *mdx* muscles showed functional recovery even 24 weeks after treatment. Surprisingly, when introduced into neonatal muscle, microdystrophin expression in a relatively small percentage of

1525-0016/$30.00